

USGS-WWDC Water Research Program Final Project Report

Treatment of Produced Water and Rare Earth Element Resource Cost-offsets, Wyoming.
Project 54, 07/01/2018 – 06/30/2019

Prepared by Charles Nye, Center for Economic Geology Research, Department 4902, University of Wyoming
Email address: cnye3@uwyo.edu
Phone: (307)-766-6804

Abstract

This study sampled 46 samples from four different Wyoming basins. These samples were analyzed for standard geochemistry, for rare earth elements, for stable isotopes, and for microbial community structure. Further, a set of tests were performed to determine how these waters might be purified to the level needed for beneficial use.

Students from the University of Wyoming were involved in each of these sample collections, analyses, and interpretations. These students presented their work and in some cases published on their findings. Many additional papers which describe this work remain in pre-publication.

The studies showed that Nano-Filtration (NF) is a good way to clean produced waters to arbitrarily high-quality, if the output is used as input to subsequent cycles. Each NF test produced 16 samples representing the feed and permeate solutions at 30-minute intervals during a 4-hour test. These samples and measurements taken during operation showed that NF was able to improve water quality without clogging the filter membrane.

The study of rare earth elements (REE) showed that an evaporite lake had concentrated all REEs, and also had a likely accumulation of the important REE europium in a non-aqueous phase. Europium is used as an additive in glasses and alloys to change photo-electric properties. The REE study also showed that one oil and gas sample had over 1ppm of the REE Cerium. These and on-going study will allow estimation of the contribution of REE to the value of water in Wyoming.

This study has initiated and enhanced relationships between: University of Wyoming, oil and gas producers, private landowners, Idaho National Laboratories, and Wyoming companies. The study has also enhanced relations within the University of Wyoming, bringing together faculty and students from the Department of Chemical Engineering, Department of Civil and Architectural Engineering, Geology and Geophysics, and the Center for Economic Geology Research. These relationships are expected to continue to benefit the University of Wyoming, the State of Wyoming, and other organizations in future work, including the WRIR project, which was made possible by this work, and dovetails its beginning with this work's end.

Progress

This work is a collection of five types of analyses to study four sample sets. These sample sets are “PRB2” from the southeastern Powder River Basin, “QD” from the northwest Laramie Basin, “DS” from the eastern Great Divide Basin, and “CH” from the northwestern Wind River Basin.

The focus of this work was on the sample set “PRB2” which was collected, analyzed, and reported in collaboration with the same industry, national laboratory, and academic groups as the “PRB” sample set which was part of the previous work which inspired this study. The other oil and gas data set “QD” was used to expand the PRB2 model to more tar-like oil and to study metagenomics in collaboration with University of Wyoming Department of Civil & Architectural Engineering. The last two datasets, called “DS” and “CH”, were of near-surface water used domestically. Metagenomics was also applied to these surface waters in collaboration with the University of Wyoming, Department of Chemical Engineering.

	Type	Geochem	REE	Microbes	SIF	NF-test	Students involved
PRB2	Oil/Gas	Yes	Yes	Yes	Yes	Yes	Shahabadi
QD	Oil/Gas	Yes	Yes	Yes	Yes	No	Shahabadi, Drogos
DS	Domestic	Yes	Yes	Yes	Yes	No	Golding and Carducci
CH	Domestic	Yes	No	No	No	No	Analytical methods class, Tanner, Strom, and SoundingSides ¹

Figure 1: The four sample sets, the analysis run on each and the students who were either financially supported or supported with samples and data.

In total these datasets contained 46 samples and four field blanks. Data produced also includes the Nano-Filtration (NF) test resulted in fractionated splits of a raw sample into feed and permeate solutions for a total of 55 splits, all of which were analyzed geochemically and show that NF can improve water quality without filter clogging.

¹ Due to weather these students were not able to attend sample collection. The analytical methods class performed analysis of all CH samples by ion chromatography.

Objectives

This work had three objectives:

1. Collect samples of produced water.
2. Analyze those samples for REE, geochemistry, isotopes, and water quality.
3. Assess the treatment of that water for beneficial use and mineral recovery.

The first objective was fully met by collection of the 46 samples from Wyoming, which almost doubled the number of samples from the previous work in Wyoming. The second was fully met in the PRB2 dataset, and less completely in the other datasets. This was because there were more samples than could be analyzed for REE analysis at INL in the time available, and because past work suggested that samples with low total dissolved solids would not contain measurable levels of REEs. The third and final objective was met for one treatment, Nano-filtration. This treatment was selected because it could improve almost any water and could be chained to reprocess its output for further improvement to produce whatever high-quality water is required.

An opportunity for expanding the work by producing custom-tailored water treatment recommendations was not achieved. However, the tested treatment of nano-filtration is widely applicable and could be used almost anywhere, making it a suitable recommendation in the absence of more attractive alternatives.

An opportunity to study the microbes associated with the water samples was not originally considered, but was achieved using the filtrate accumulated on filter papers after the sample has been filtered. (These filter papers would otherwise have been discarded.) This metagenomics work involved two different groups in UWyo's College of Engineering and Applied Science.

Likewise the opportunity to sample domestic as well as produced waters was not originally envisioned as part of this work, but its addition allowed a valuable insight to water quality in the end use of human domestic drinking water. The CH sample set in particular will serve UWyo well in future studies as it developed an important relationship with a supportive community in the Wind River Basin. This community is eager to provide in-kind support for University of Wyoming projects, and previously worked with architecture students and Dr. Gardzelewski in the College of Engineering and Applied Science. That successful relationship was maintained during this work, and community representatives have reiterated their interest in supporting University of Wyoming fieldwork and other activities.



Figure 2: Two samples being filtered. The rust-colored sample on the left is typical of the PRB2 sample set and the clear sample on the right is typical of the QD sample set. When the QD sample set was filtered a coffee filter was used to separate the oil-tar from the produced water. This filter had been soaked in toluene, dried, and microwave sterilized to ensure it did not affect the microbial rRNA extracted as part of the Metagenomic methods.

Methodology

General sampling method

CEGR's standard methodology for water samples was followed with minor modifications.² All water samples were collected from either a separator (PRB2), a spigot/low-pressure line (CH, QD), or surface run-off (DS). They were collected in sterile 500 mL LDPE bottles, rinsed with sample, filled to overflowing, sealed using screw caps to prevent oxygen intrusion, and stored on ice in the field. All samples reached a 4°C refrigerator in the lab within 24 hours of sample

² Nye, C., Quillinan, S., McLing, T. L., Neupane, G., Mclaughlin, J. F. and Bagdonas, D. A. (2016) Aqueous Rare Earth Element Patterns and Concentration in Co-produced Brines and Industrial Ponds, Wyoming. GSA Abstracts with Programs. <http://dx.doi.org/10.1130/abs/2016AM-285615>

collection. Samples for cation analysis were preserved with trace-metal grade HNO₃. Water samples for chemical and microbial analyses were filtered through a sterile 0.2µm filter. Field measurements included temperature, pH, ORP, and conductivity using a Myron Ultrameter II.

Geochemical method

Filtered water from both acidified and non-acidified splits was analyzed for cations and anions according to EPA 200.8, 200.7, and EPA 300.0, respectively. Alkalinity was determined using method A2320 B on the same split as anions.

Rare Earth Element method

One 500ml bottle of each PRB2 sample was sent to Idaho National Labs. These analyses were performed following the modified method of McLing 2014³ used in past work.⁴ The method of McLing (2014) involves selective concentration of REEs by selective resin column chemistry, then measurement by ICP-MS. This method removes the mass-interference problem, and reduces salt-content so REEs can be measured at better accuracy and precision than in the raw sample.

Metagenomic method

The filter was preserved so that rRNA could be isolated with the Qiagen PowerWater Kit. 16S v3-v4 rRNA was sequenced using the Illumina MiSeq platform, and initial raw reads quality was assessed using FastQC. Qiime2 was used to denoise and dereplicate the reads. They were then compared with the Greengene 13.8 database and assigned taxonomy using Qiime2. This method was described in two other works both led by students who received samples as a result of the project.⁵

³ McLing, T., Smith, W., & Smith, R. (2014). Utilizing Rare Earth Elements as Tracers in High TDS Reservoir Brines in CCS Applications. *Energy Procedia*, 63, 3963-3974.

⁴ Quillinan, Scott., Charles Nye, Mark Engle, Timothy Bartos, Ghanashyam Neupane, Jonathan Brant, Davin Bagdonas, Travis McLing, and J. Fred McLaughlin. "Assessing rare earth element concentrations in geothermal and oil and gas produced waters: A potential domestic source of strategic mineral commodities", Final Report to U.S. Department of Energy, Geothermal Technologies Office, Project Number EE0007603. U.S. Department of Energy Geothermal Data Repository, Submission #1125, Chapter 2 "Sample Collection and Library Selection", (2019). Accessed from <https://gdr.openei.org/submissions/1125>

⁵ Golding, Aspen, Nunzio Giorgio Carducci, Charles Nye, and Karen Wawrousek. (2019) "Microbial Communities Composition in Water Samples from a Geothermal Well". Undergraduate Research Day, University of Wyoming, Laramie, Wyoming, April 27, 2019.

Nunzio Giorgio Carducci, Aspen Golding, Charles Nye, and Karen Wawrousek. (2019) "Microbial Community Composition in Water Samples from a Geothermal Well". Rocky Mountain Branch of the American Society of Microbiology, May 4, 2019.

Isotope method

UWSIF ran isotopic analysis with Job codes “017 GC-IRMS” and “024 CRDS”. Carbon isotopes were measured following acidification leading to evolution of all dissolved inorganic carbon (DIC) as CO₂. The DIC was measured using a GasBench attached to an isotope ratio mass spectrometer. Hydrogen and Oxygen isotopic compositions of water were measured using a Picarro L2130-I Cavity Ring Down Spectrometer. All isotopic compositions are reported in standard δ notation. Carbon isotope ratios are reported relative to Vienna Pee Dee Belemnite (VPDB) and hydrogen and oxygen isotope ratios are reported relative to Vienna Standard Mean Ocean Water (VSMOW).



Figure 3: The NF test-apparatus, showing the conical reservoir below, the instrumentation above, and the NF membrane cell in white (with blue lettering) at the very top.

Nano-filtration (NF) experimental method

The NF experiment used the test-apparatus shown in Figure 3. This equipment is part of the Center for Excellence in Produced Water Management (CEPWM). Over the course of half a day, permeate flux, and pressure were recorded at regular intervals. Permeate flux is reported as clean water flux, (L/m²h or LMH at a specific pressure of 110 psi) versus time. Normalized flux is the

permeate flux/pressure (110 psi). Change in the permeate flux/normalized flux vs time shows how fast clean water is passing through the membrane. Another important consideration is how much REEs or other elements pass through the membrane into the permeate stream. This is called membrane rejection ($R = 1 - \text{concentration in permeate} / \text{concentration in feed}$; feed is the initial solution), and must be measured after the experiment using aliquots of permeate and feed solution collected every 30 minutes. The first three of these samples are seen in Figure 4 in the rack on the table.

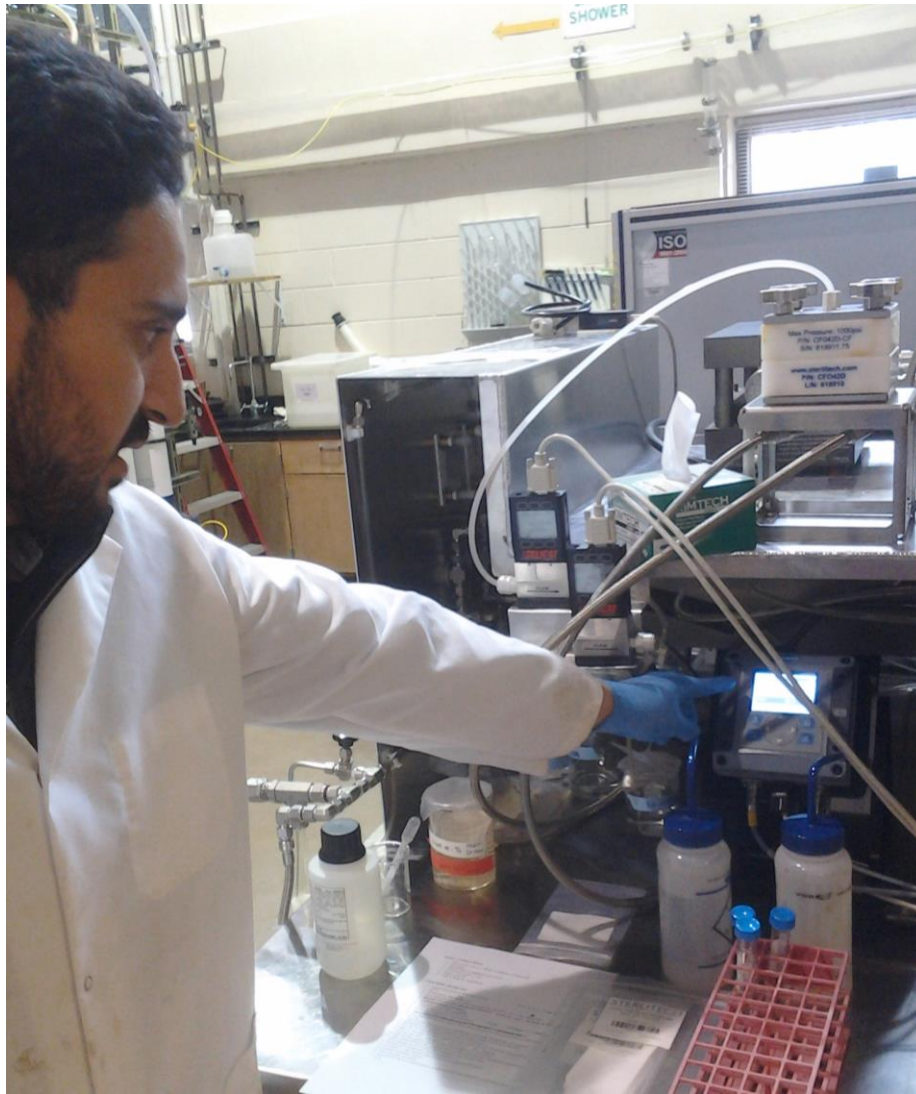


Figure 4: M. Shahabadi indicates the pH meter used to guide the addition of HCl to the circuit. Acidic conditions maintain the Zeta potential on the NF membrane. New membranes are visible on the table, and the cell they are loaded into is again visible at the very top of the apparatus.

Principal Findings

PRB2: Geochemical findings

The PRB2 samples come from the Powder River Basin in northeast Wyoming. The Powder River Basin is an asymmetric syncline bounded by the Big Horn Mountains, Laramie Range, and Black Hills. The basin drains into Montana. The basin's axis is off-center to the east and runs approximately north-south. All samples in this study were from the shallow eastern limb of the basin or on the axis. The sampled area encompasses the towns of Wright and Bill, Wyoming.

As seen in the PRB dataset which predates this study⁶, the PRB produced waters are all sodium-chloride type. This is a common feature of ground waters whenever their salt content approaches that seen in saline ocean water (~30,000 mg/l). Past work showed that there was minimal sulfate content, which is the case in the present study as well, with only three samples from PRB2 containing detectable sulfate, all less than 80 ppm. In addition to sodium and chloride, there are minor amounts of carbonates, bromide, calcium, and strontium. Potassium is significant in samples from the more northerly Turner and Frontier formations. One sample from the Mowry shale contained significant nitrates, which may evidence human activities boosting microbial activity in that location.

In general in the PRB2 waters, the low concentrations of heavy metals and other substances hazardous to humans indicate that the monovalent sodium chloride content and residual hydrocarbons are the primary obstacle to putting this water to beneficial use. This conclusion allowed the CEPWM to narrow its study of treatment technologies to Nano Filtration (NF).

The PRB2 waters reached the sample-collection point on the separator at a warmer temperature (35C average, range 20C to 43C) than the other samples. Like the other produced water samples from QD, these samples are neutral to slightly acidic. The Oxygen Reduction Potential (ORP) is near that of a standard electrode (+/- 0.1 s.u.), in the center of the stability field of water. However, of these samples the more reduced waters tend to be found in the more northern sample areas. The more reduced samples come from the Parkman formation, suggesting this formation's lithology contains reducing mineral species, which are reflected in the water from the Parkman. The Parkman also has lower overall salt content, and the lack of redox-buffering reactions could explain the water's reduction.

⁶ Quillinan, Scott., Charles Nye, Mark Engle, Timothy Bartos, Ghanashyam Neupane, Jonathan Brant, Davin Bagdonas, Travis McLing, and J. Fred McLaughlin. "Assessing rare earth element concentrations in geothermal and oil and gas produced waters: A potential domestic source of strategic mineral commodities", Final Report to U.S. Department of Energy, Geothermal Technologies Office, Project Number EE0007603. U.S. Department of Energy Geothermal Data Repository, Submission #1125, Chapter 4 "Aqueous Sample Analysis", (2019). Accessed from <https://gdr.openei.org/submissions/1125>

PRB2: Rare Earth Element findings

The PRB2 samples were analyzed with a triple quad Thermo Scientific iCAP TQ ICP-MS, operated in oxygen addition mode. The analyses were provided by Idaho National Labs, and are an early report which has not been as fully QA/QCed as less rushed analyses from INL.

In produced water samples with high europium content samarium and gadolinium are sometimes also present at higher concentrations. Past work on the PRB sample set, which predates this work, found a gadolinium anomaly, which was much larger than that for samarium. These anomalies appear to occur again in the PRB2 sample set, but would require normalization to show conclusively (Figure 5). In the PRB2 data set there does not appear to be a selective HREE anomaly like what was found in the PRB dataset. The highest non-LREE and non-europium samples are PRB2-77 and PRB2-78. These samples come from the southern portion of the PRB2 sample set around Bill, WY and are the only two Frontier samples in that area. Two samples show pronounced cerium anomalies, which could be related to the valence of Ce which can be either 3+ or 4+.

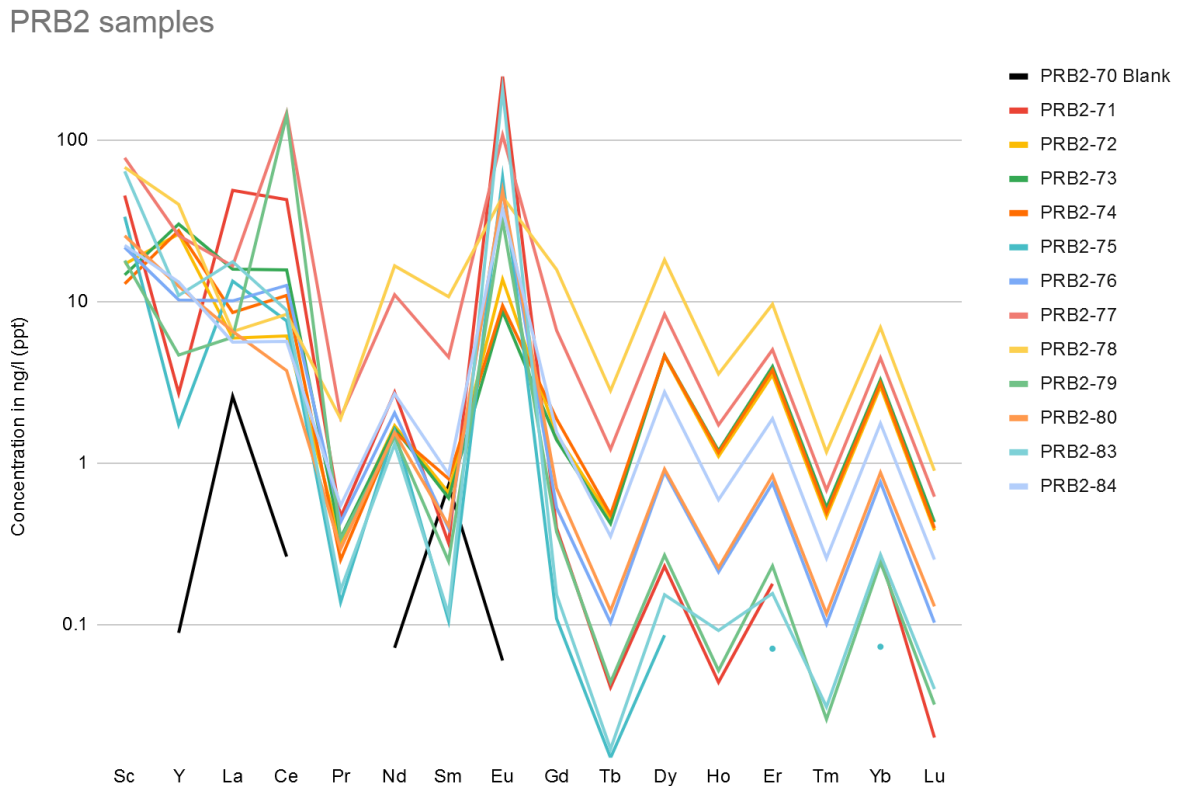


Figure 5: Non-normalized rare earth element results from the PRB2 sample set, showing the europium anomaly in all samples.

PRB2: Metagenomic findings

The metagenomic data for PRB2 has been completed and is available through the College of Engineering and Applied Science. These data are being prepared for a manuscript and will include comparisons to other Wyoming basins, and internal comparisons to different parts of the basin, and the geochemistry. These data should reveal change over time and sampling-induced noise through partial overlap with the PRB sample set.

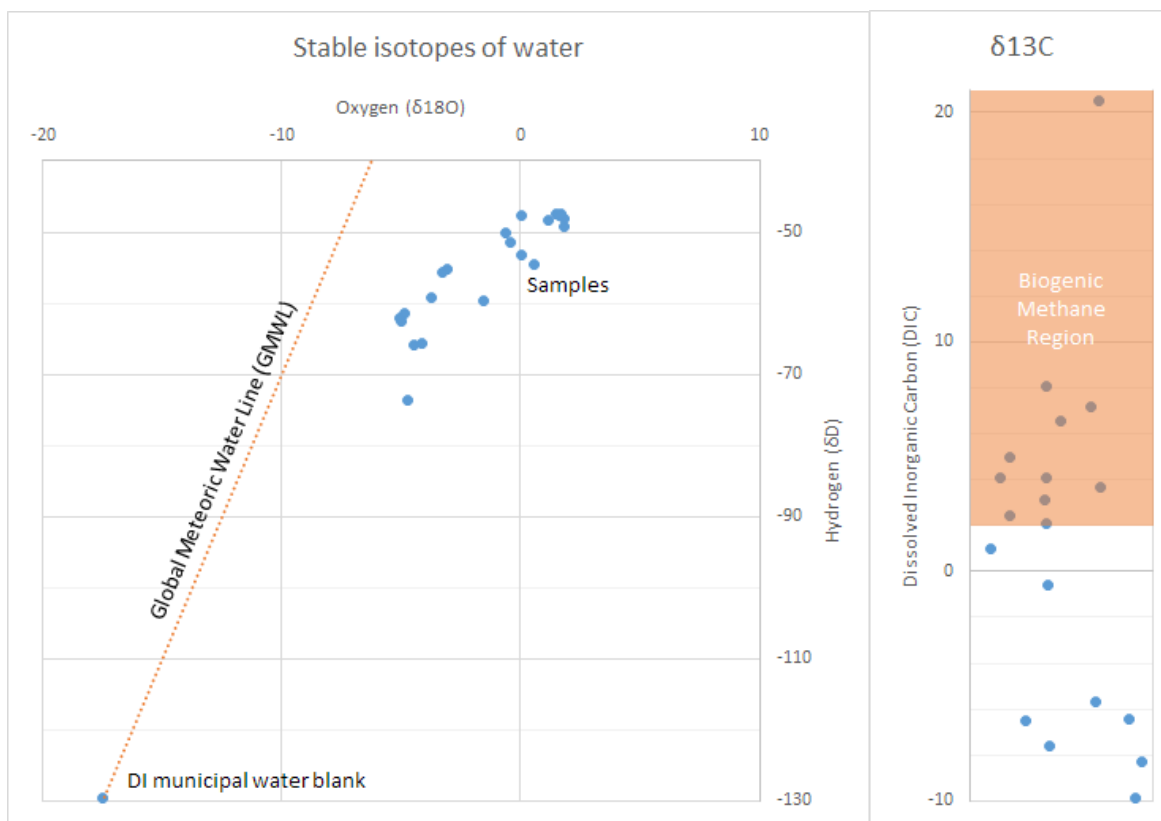


Figure 6a and b: The samples from PRB2 cluster in the near-zero area where most Wyoming oil and gas samples reported in the previous work cluster.⁷ Six samples overlapped between the pre-existing PRB sample set and the new PRB2 sample set collected in this work. More interesting is the behavior of the PRB2 samples in carbon stable isotopes, which indicates methanogenesis has occurred in more than half the samples.

⁷ Quillinan, Scott., Charles Nye, Mark Engle, Timothy Bartos, Ghanashyam Neupane, Jonathan Brant, Davin Bagdonas, Travis McLing, and J. Fred McLaughlin. "Assessing rare earth element concentrations in geothermal and oil and gas produced waters: A potential domestic source of strategic mineral commodities", Final Report to U.S. Department of Energy, Geothermal Technologies Office, Project Number EE0007603. U.S. Department of Energy Geothermal Data Repository, Submission #1125, Chapter 4 "Aqueous Sample Analysis", (2019). Accessed from <https://gdr.openei.org/submissions/1125>

PRB2: Stable O, C, and H Isotope findings

All PRB2 samples have oxygen and hydrogen isotope values in the region previously seen for oil and gas produced waters (2,-45 to -5,-75). These values are distinct from the QD and DS samples as described in later sections of this report. The carbon isotope results show that over half the samples are in the region which normally indicates removal of light carbon by methanogenic bacteria. The residual heavy carbon has a DIC value of +2 per mil or higher (heavier isotopes) when compared to Vienna Pee Dee Belemnite (VPDB). Samples outside the colored region on Figure 6b could still be significantly influenced by biogenic methane production but either to a lesser degree, or subsequently mixed with a more typical groundwater of DIC around -12 per mil. Values as high as +2 can be a result of exposure and equilibration with carbonate rocks.

QD: Geochemical findings

At the QD sample site in the Laramie Basin, there are two types of waters. These waters are co-produced with heavy oil and come from wells inside a 1 mile-diameter circle. The waters form two distinctive groups, one of high sulfate and one of high carbonate. In this work, these two distinctive groups are called Type S waters (n=6), and Type C waters (n=5) respectively. All samples were collected and analyzed by the same protocols. The QD set were collected in a single day. This control yields a dataset with high control over introduced error, allowing description of nuanced processes.

Type S waters have two orders of magnitude more sulfate than Type C waters. Type S waters are characterized by a more reducing environment (ORP averages -269mV) and a more saline chemistry averaging 4172 ppm total dissolved solids. Type S waters have higher concentrations of most analytes, especially (ordered from greatest significance to least): strontium, calcium, magnesium, potassium, ammonia, chloride, sodium, bromide, boron and silicon.

Type C waters are more dilute, and contain at most 18 ppm sulfate, resulting in them appearing as Na-CO₃ waters despite having only slightly greater alkalinity than Type S waters in absolute terms. The type C waters are not only more acidic with an average pH of 5.6 units but also more oxidizing with an ORP of -139mV. Type C waters have significantly more barium and also often more fluoride. The low sulfate content of Type C waters is almost certainly responsible for the increase in observed barium as BaSO₄ is a common irreversible precipitate.

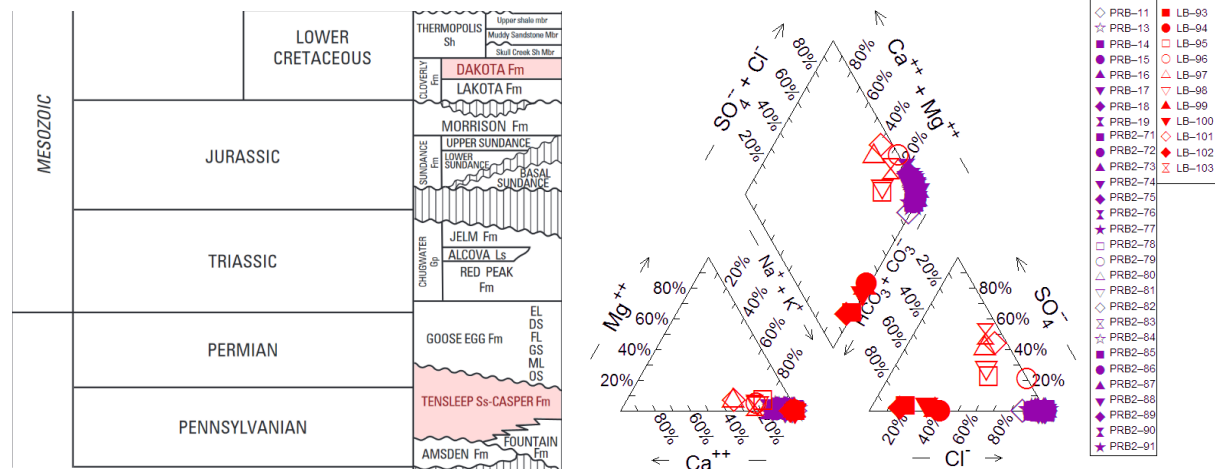


Figure 7: The C-type and S-type sample in the QD sample set align with two distinct time periods in the lower Cretaceous and the Permian-Pennsylvanian. These have two different water chemistries which are unlike the PRB and PRB2 samples as shown on the piper diagram.

The deeper Tensleep Formation is the source of Type S samples, and the shallower Sundance/Muddy formations is the source of Type C samples. This clear-cut correlation between formation and water type was not known in advance of analysis, so the distinction shows the value of geochemistry in tracing water from subsurface formations. Results from one sample illustrates the power of the geochemical fingerprint. One sample was collected from a well listed as completed in the Muddy Formation but had water of Type C. This apparent exception to the rule was resolved when subsequent re-checking revealed that the well in question had been re-completed in the Tensleep Formation, rendering the documentation out of date. With this apparent conflict resolved, it is possible to identify the source formation of all water samples based on their water type and shows the power of this geochemical approach

QD: Rare Earth Element findings

One sample from the Tensleep formation, QD-96, has very high cerium content (over 1ppm) and significant concentrations of the other REEs. Two samples from the shallower formations QD-93 and QD-94 have intermediate concentrations of REEs. The vast majority of QD samples are low concentration. Only three QD samples exhibit the europium anomaly normally seen in oil and gas produced water samples.

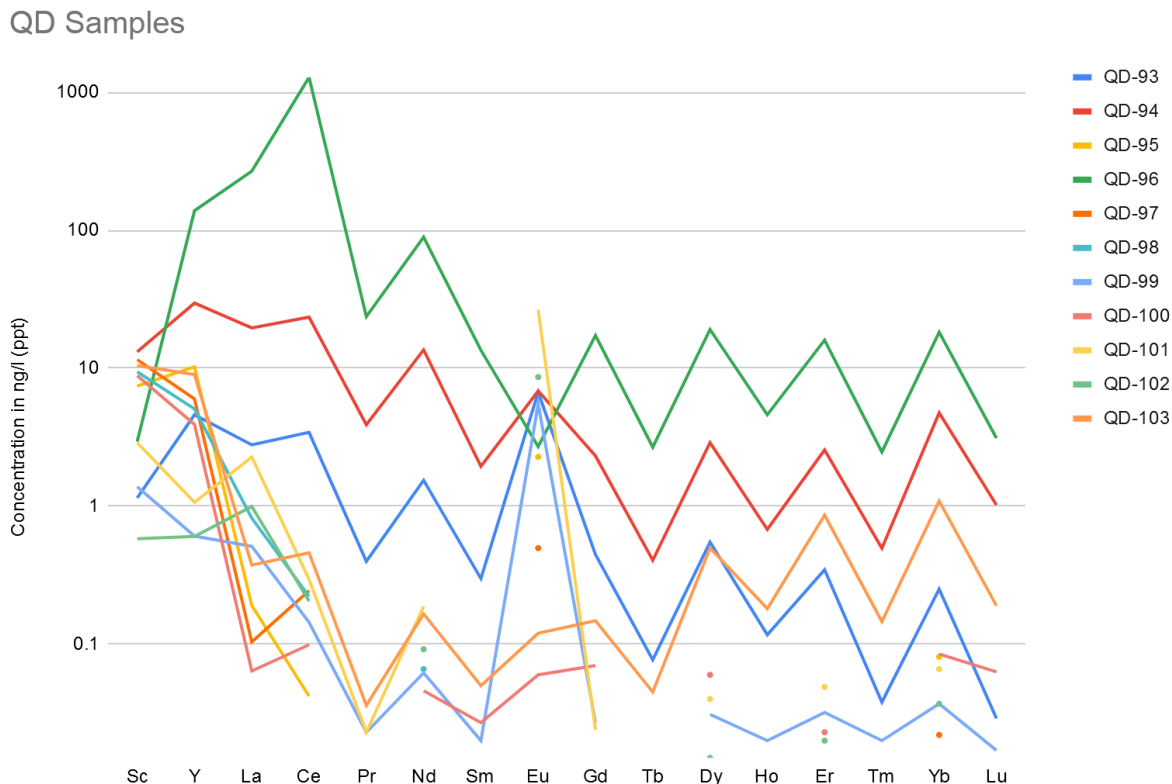


Figure 8: Some QD samples share common features with PRB2 samples, such as positive europium anomalies. The large amount of cerium in one of these samples exceeds 1ppm.

QD: Metagenomic findings

Evaluation of the microbial community in the QD samples is not yet complete. The work will identify and compare the microbial communities present in crude oil samples and the water samples. This comparison of water and tar was only possible within the QD set as the oil-tar could be readily separated from the water fraction as seen in Figure 2. For each sample microbial rRNA will be extracted from the oil-tar and the water fraction, and analyzed by 16S rRNA gene sequencing. This will reveal if microbial communities present in different phases are different. It could indicate a need to modify Microbial Enhanced Oil Recovery (MEOR) and water management strategies. The graduate student involved plans to produce a journal article about the findings.

QD: O, D, and C Isotope findings

Most samples from the QD data set have carbon values in the region for normal groundwater (-15 to -5 per mil). There are three samples in the microbial methane region, and one near 0 which is ambiguous. Figure 8 shows the QD isotopes as orange triangles.

The isotopes of water are in the same area that most laboratory blanks are. Because these blanks were made at the University of Wyoming, which sources its water from the Laramie Basin aquifers they have very light hydrogen and oxygen ratios. The QD sample set which also comes from the Laramie Basin plots in the same area as these very light-isotope enriched waters.

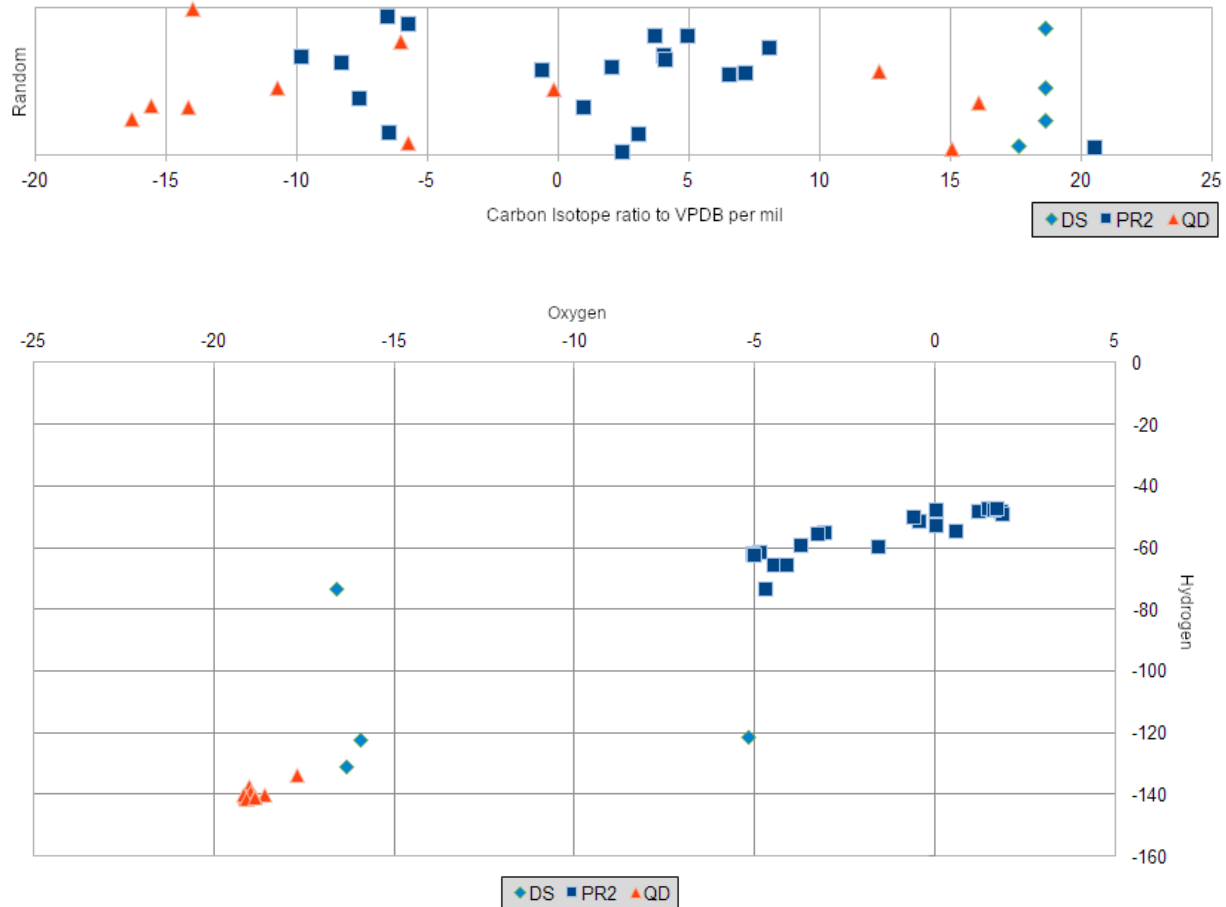


Figure 9: Isotope results for carbon stable isotope ratio (top) and hydrogen-oxygen stable isotope ratio (bottom) for the DS, PRB2, and QD samples. The carbon data points are 1-dimensional but given a random Y-axis offset for visibility. Oxygen and Hydrogen standardized to VSMOW and show clustering by sample set. Evaporation could be responsible for those samples' spread.

DS: Geochemical findings

Sampling at DS was performed with brown glass bottles because the researchers were told the water was hot. A smaller volume of water was collected from the run-off stream, which connects the pool to the lake at the DS site, because only 12 brown glass bottles were available, and one was lost in the muddy lakeshore. This reduced the geochemical analyses possible for that sample.

In most analytes the abandoned well and the lake form endmembers and the pool and/or stream have intermediate values. Figure 10 shows this trend.

	pH (units)	Conductivity (mS/cm)	Temperature (°C)	ORP (mV)
Wellhead	7.40	4.70	31.1	-36
Well Pool	8.15	4.18	29.4	8
Run off Stream	8.30	11.3	27.2	22
Bull Spring Lake	8.81	80.0	17.7	13

Figure 10: Field measurements collected at the time of sampling. Most show a steady change as the water travels to the lake. The measurements that do not follow a pattern of steady change along the water's flow path are the conductivity in the well pool (which is within error), and the ORP in the evaporative lake. These field parameters are visualized on Figure 18.

The acidic low TDS conditions in the well change smoothly to more basic high TDS conditions in the lake. This could be a result of cooling, or the accumulation of species which buffer the lake to near the pH for carbonate-bicarbonate equilibrium. The ORP shows oxidation mostly occurs during the turbulent transport step in the stream. While the lake is oxidized its lower turnover may produce slightly more reduced conditions. These relative changes should not overshadow the similarity of these waters to typical surface conditions.

The geochemistry of these waters was limited as explained above to just the Well, Pool, and Lake. Figure 10 shows that while the geochemistry does not change too much between the Well and Pool, the effects of evaporation in the lake significantly change all analytes by as much as two orders of magnitude. The apparent loss of concentration in some analytes is most likely due to dilution as the enriched species accumulate.

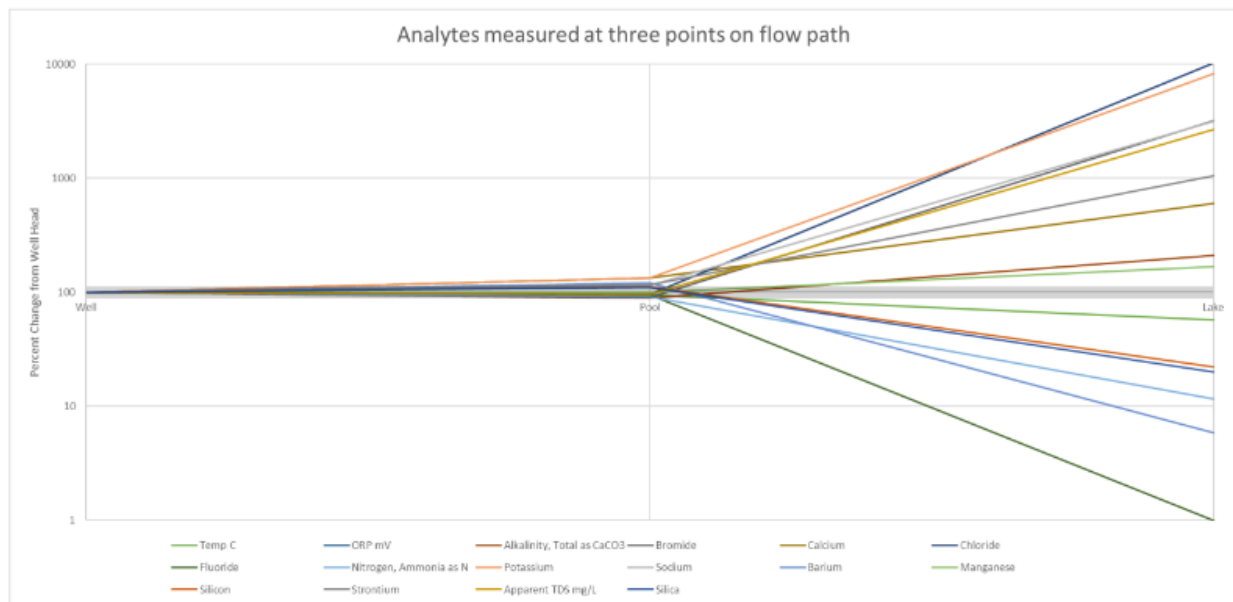


Figure 11: Geochemistry changes between the well, the pool, and the lake. The Y-axis is the percent change from the wellhead sample. The X-axis shows the three sample locations as water flows from the well to the lake. Change is minimal between the well and the pool, and very great between the pool and the lake.

DS: Rare Earth Element findings

The DS samples form a sequence as the water from the abandoned well flows out of the well, into a pool, down a run-off stream, into an evaporative lake. The unnormalized data is presented on Figure 12 below, and in the appendix. There is very little change among the first three points (note log scale) which have very similar patterns and concentration. The water, like other oil and gas produced waters has a strong positive Europium anomaly which has previously been interpreted as the change of europium's valence. The lake-sample is significantly different from the first three samples in this flow-path study. In the lake-sample europium lacks the anomaly normally seen in oil and gas produced waters. The lake samples are also generally higher concentration of all REEs, which agrees with concentration of all species in the lake as a result of evaporation. The increased exposure to oxidized conditions, or halophile microbes which maintain conditions on the surface of their cells unlike those conditions in the rest of the lake may explain the europium anomaly. Future work could seek out the phase, likely solid, which now holds this europium, possibly at useful concentrations.

DS sample set

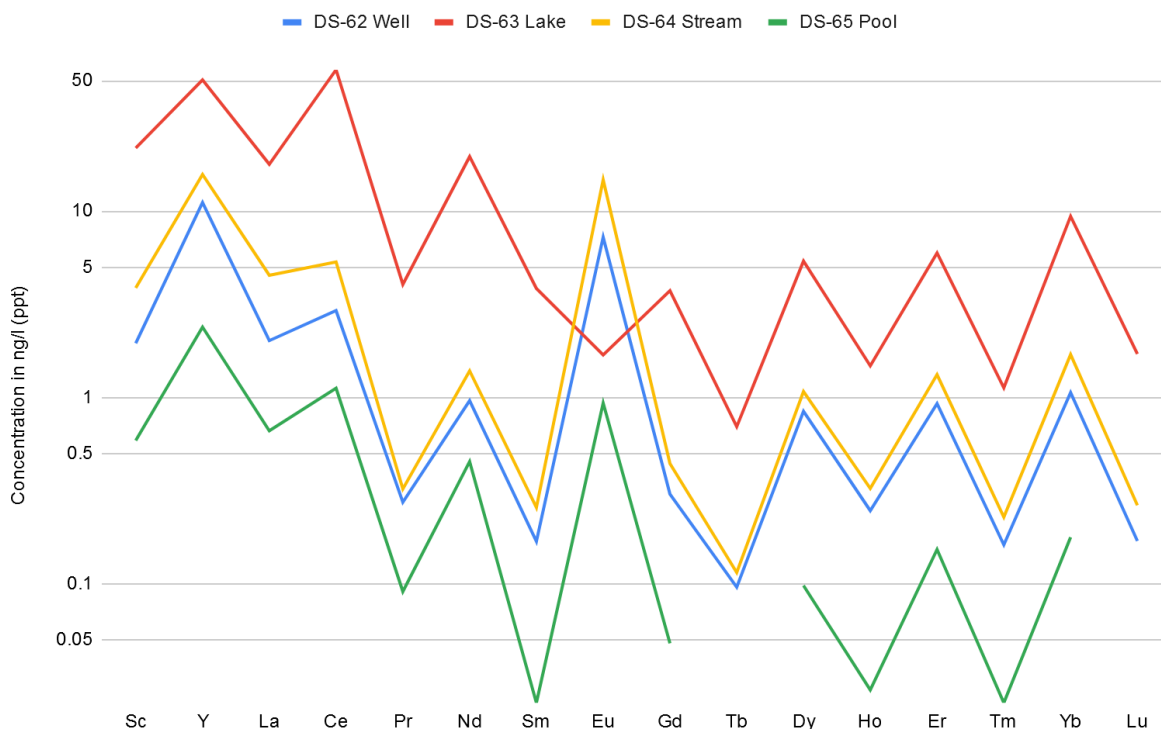


Figure 12: REEs in the DS sample set are all fairly similar in structure and concentration, but the evaporative lake sample (DS-63, shown as the red line) is significantly different.

DS: Metagenomic findings

Completed September 16, 1925, the wildcat oil well at the DS sample site was drilled and abandoned. It has remained open and flowing ever since. The well site provided the only samples from an endorheic basin, a basin which has no outlet, so all water that leaves the basin does so by evaporation. Water samples were taken directly from the well, from a pool on the surface next to the well, halfway down a run-off stream between the pool and the lake, and directly from the lake. 16S rRNA gene sequences, which indicate prokaryotes, and 18S rRNA gene sequences, which indicate eukaryotes, were analyzed to classify and characterize the microbial communities present in each of these four samples.⁸

⁸ Whitman, William B., et al. *Bergey's Manual of Systematics of Archaea and Bacteria*. , doi: 10.1002/9781118960608.

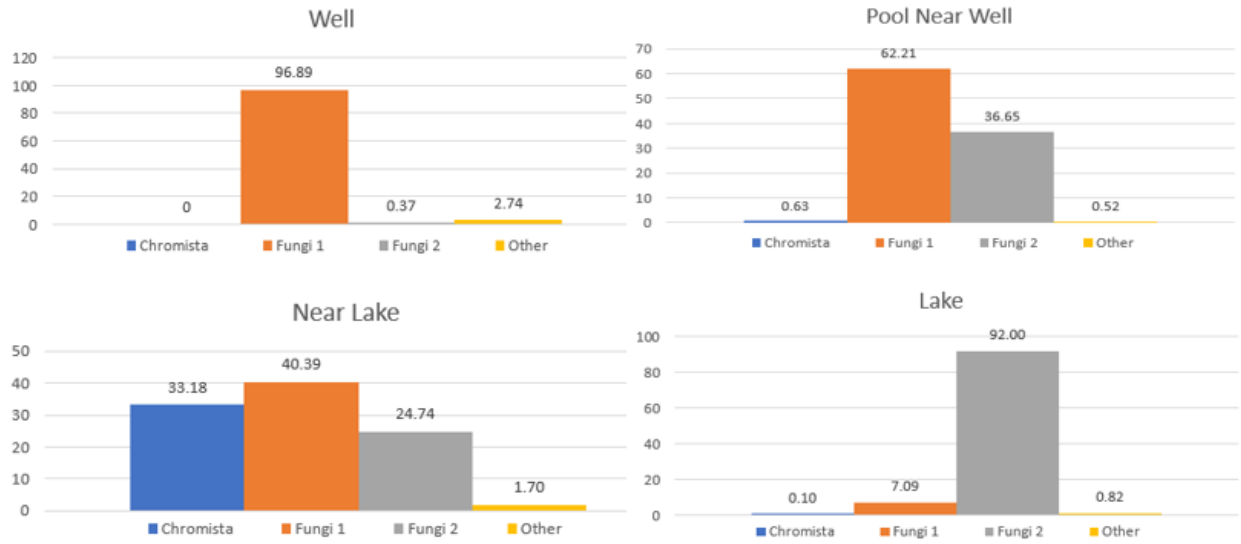


Figure 13: Diversity of fungi changes from one endmember in the well to another in the lake. The middle steps of the run-off stream and the pool represent intermediate transitions between the endmembers.

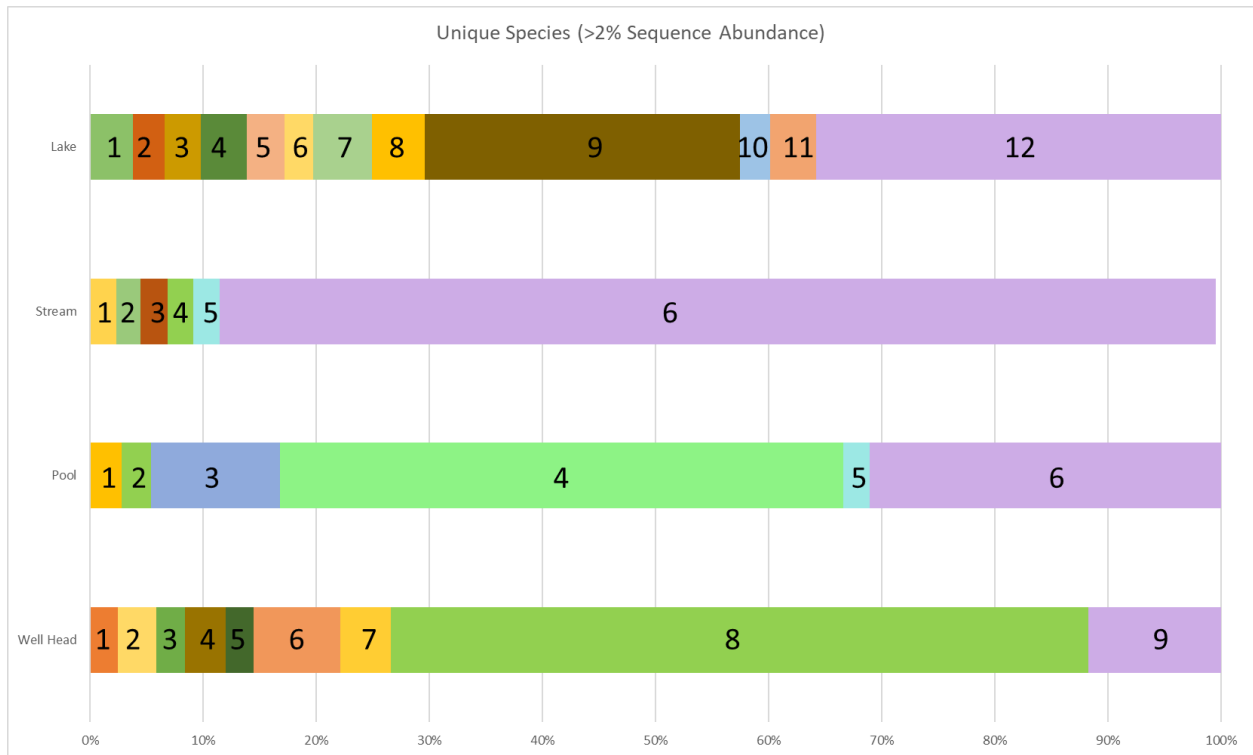


Figure 14: Bar chart breakdown of the most prominent species in four water samples. Percentages are based on the sequence frequency of each taxa-species divided by the total number of sequences in the sample.

Location	Taxonomy	Description	Location	Taxonomy	Description
Well Head			Pool		
1	k__Bacteria	N/A	1	f__Rhodobacteraceae (P1, L8)	Diverse; includes photoheterotrophs and chemorganotrophs; require Na ⁺ for growth
2	p__OD1 (Parcubacterium)	Anoxic environment; severely reduced metabolic capabilities	2	g__Hydrogenophaga (WH8, P2, S4)	Aerobic; oxidizes H ₂ with CO ₂ as a carbon source
3	o__ASSO-13	N/A	3	g__Flavobacterium	Chemorganotrophic; reduces nitrate to nitrite
4	f__Rhodocyceae	Diverse; anoxygenic photoheterotrophs; plant-associated nitrogen-fixing aerobes; carbon-degrading species; anaerobes	4	g__Arcobacter	Chemorganotrophs; can tolerate air
5	g__Azovibrio	Microaerophilic; chemorganoheterotrophic; strictly respiratory; fix N ₂	5	Methylobacter luteus (P5, S5)	Obligate user of methane for carbon and energy; requires oxygen; neutrophilic
6	Dechloromonas fungiphilus	Facultatively anaerobic, strict respiratory metabolism; chlorate and perchlorate reduced to chloride; O ₂ or sometimes nitrate as e ⁻ acceptor	6	Other	
7	g__Thiothrix	Aerobic or microaerophilic; Species vary from facultatively autotrophic, chemorganotrophic, mixotrophic; found in sulfide-containing water			
8	g__Hydrogenophaga (WH8, P2, S4)	Aerobic; oxidizes H ₂ with CO ₂ as a carbon source			
9	Other				

Location	Taxonomy	Description	Location	Taxonomy	Description
Stream			lake		
1	o__Bacteroidales	Facultatively anaerobic or saccharolytic	1	f__Cryomorphaceae	Strictly or facultatively anaerobic; chemorganotrophy; most genera require seawater salts to grow
2	o__Clostridiales	Phenotypically, chemotaxonomically, physiologically and ecologically diverse.	2	f__Flavobacteriaceae	Mainly aerobic growth; can reduce nitrates; inorganic nitrogen is also used
3	g__Rhodobacter	Photoheterotrophic growth under light anoxic conditions	3	g__Psychroflexus	Strictly aerobic; chemoheterotrophic; strains require Na ⁺ for growth; stenohaline or halotolerant
4	g__Hydrogenophaga (WH8, P2, S4)	Aerobic; oxidizes H ₂ with CO ₂ as a carbon source	4	g__Psychroflexus	Strictly aerobic; chemoheterotrophic; strains require Na ⁺ for growth; stenohaline or halotolerant
5	Methylobacter luteus (P5, S5)	Obligate user of methane for carbon and energy; requires oxygen; neutrophilic	5	g__KSA1	Aerobic
6	Other		6	o__Stramenopiles	N/A
			7	c__ZB2	Anoxic environment; severely reduced metabolic capabilities
			8	f__Rhodobacteraceae (P1, L8)	Diverse; includes photoheterotrophs and chemorganotrophs; require Na ⁺ for growth
			9	g__Rhodobaca	Phototrophic; aerobic respiration; requires growth factors
			10	g__Halomonas	Chemorganotrophic. Respiratory metabolism. Nitrate reduced to nitrite.
			11	c__Mollicutes	Most are facultative anaerobes but some obligate anaerobes
			12	Other	

Figure 15: Four keys for describing the numbered taxa in Figure 14. Kingdom, Phylum, Class, Family, Order, or Genus is represented by the first letter of the name. In some cases labeled “N/A” more research is needed to determine the taxa’s role in the community.

The four samples show increasing microbial species diversity as the water leaves the well, and becomes more and more oxidized, however, the extreme salt conditions in the evaporative lake reduce diversity because they strongly favor halophilic microbes. Figure 13 shows this change occurring for fungi. Figures 16 and 17 show the change for all 16S and 18S microbial species.

The proportions of microbes of the most common species (>2% by sequence abundance) are shown visually on Figure 14 below, and described on Figure 15. In the well-head sample anaerobic species dominate the community, and to some extent in the pool water samples near the well head. This aligns with the low oxidation-reduction potential (ORP) in these samples. As the ORP of the water increases, the number of anaerobes decreases and the count of aerobes increases. Finally, in the evaporative lake, halotolerant species are present because they are most able to survive in the high-sodium, high-magnesium environment.

16S rRNA	Well Head	Pool	Stream	Lake
Simpson Diversity Index	0.607	0.734	0.992	0.905
Shannon Diversity Index	1.689	2.431	5.166	3.355

Figure 16: Simpson and Shannon diversity indexes for 16S rRNA

For the 16S rRNA, the Simpson and Shannon diversity values support the observation of increasing biological diversity as the water's oxygen concentration increases and its temperature decreases. The diversity likely decreases slightly in the lake due to the extremely high salt concentrations. The species present in each sample correspond well to the geochemical analysis as well. We see halotolerant species in the evaporite lake and anaerobes in the well head sample.

18S rRNA	Well Head	Pool	Stream	Lake
Simpson Diversity Index	0.061	0.469	0.666	0.149
Shannon Diversity Index	0.181	0.480	0.856	0.469

Figure 17: Simpson and Shannon diversity indexes for 18S rRNA

The results from the 18S rRNA analysis did not reveal much about the characteristics of the eukaryotic microbes, and therefore definite conclusions cannot be drawn from the data. From the Simpson and Shannon Diversity Indices, the well head is the least diverse environment and the stream near the lake is the most diverse environment. To that extent it support similar conclusions to the 16S rRNA.

DS: Isotope findings

The analytes shown in Figure 18 are generally stable over the ~3 feet of distance water travels when it splashes out of the wellhead and into the well pool. After ~50 feet of travel to the mid-point of the runoff stream, conductivity has significantly changed, as has temperature. In the lake, almost all analytes have deviated very far from the well head values, but surprisingly stable isotopes of carbon remain nearly constant.

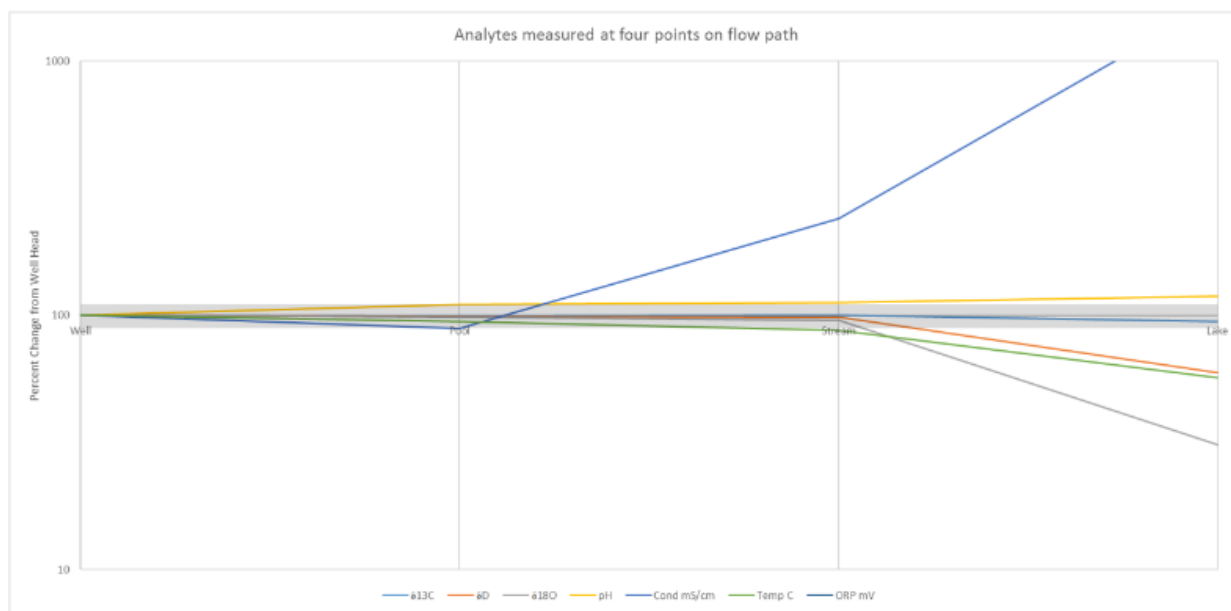


Figure 18: Isotope and field parameter changes between the well, the pool, the stream, and the lake. The y-axis shows the percent change from the wellhead sample, and the x-axis the four points at which these analytes were measured as water flowed from the wellhead to the lake.

CH: Geochemical findings

These samples were collected in late February 2020 from domestic and agricultural wells northwest of Crowheart, Wyoming. These wells and natural spring samples were collected in two aliquots, one for use by students in Janet Dewey’s Geochemical Analytical Methods Class, and one for formal analysis under the Center for Economic Geology Research’s (CEGR’s) standard procedure.

All CH water samples are lower salinity than the produced water and hydrocarbon samples CEGR usually analyzes. The air temperature was near to just above freezing on the day of collection, and samples were a mean of 7.5 degrees Celsius above freezing at the time of collection. This agrees with the expected temperature moderation provided by 25 feet to 150 feet of soil and regolith overburden. All CH samples have high oxidation-reduction potential (with one exception) which agrees with an unconfined shallow groundwater aquifer system recently recharged with precipitation. This oxidized environment is reflected in the low sulfate content of most samples. All CH samples are slightly basic, with a pH near 8. This is consistent with a carbonate-buffered system with non-urban rainwater recharge.

The following analytes were either not detected, or detected at concentrations very close to the analytical instrument's detection limit in all samples: nitrite, bromide, phosphate, ammonia, aluminum, arsenic, molybdenum, and lithium. The following discussion of the results compares the samples, and draws out their slight differences. This should not overshadow the fact that all samples are very similar to each other, and of much higher water quality than CEGR normally deals with.

Sample CH151 is slightly saltier than sample CH152 downriver to the east. This is probably due to CH152 being fed from recently melted water, and CH151 drawing from a slightly deeper, older reservoir which has had more time to pick up salts from the rock. The nitrate content of CH151 water is the highest found in this study, but should not be of concern. At higher concentrations, nitrate and nitrite (which was not detected) can support the growth of microbes. In some cases, these microbes can degrade water quality, although there is no evidence of that here. CH152 has higher sulfate content than expected from its ORP. This is probably due to the influence of plants, cows, etc. in contact with atmospheric air at the surface, near where the sample was collected. Such sources could contribute sulfate without significantly changing ORP. The samples are otherwise typical of this sample set.

The CH153 sample is typical of this sample set. However, samples CH154 and CH155 are atypical.

These two samples have more reduced conditions as evidenced by the lower ORP, which is almost negative in CH155. As expected, sulfate is higher in CH154, and the highest recorded in this sample set in CH155. This last measurement agrees with the rotten-egg smell from that sample point. The smell may be a result of trace amounts of hydrogen sulfide exsolving from the water. Humans are very sensitive to hydrogen sulfide, and can detect it well below dangerous concentrations. Sulfide was not measured in this study, but can be assumed to be in equilibrium with sulfate. As the smell was present but faint, the concentration is probably well below 0.1ppm. Hydrogen sulfide is of particular concern because at low concentrations ~5ppm it overloads the human nose and ceases to be detected, leading to an incorrect feeling of safety.

The other atypical features of these CH154 and CH155 are seen in their iron, sodium, and barium cations. CH154 is the only well with detectable iron content, which agrees with the age of this well, and degradation of iron wellbore pipe with time. Both samples have elevated sodium which seems to be associated with the sulfate. This may indicate the wells were completed: 1) in an evaporite bed, 2) with less robust cement - if they were cemented, 3) in proximity to sulfide minerals like pyrite and reactive volcanic minerals, or 4) for CH155 only, were passed through a water softener - See CH159 and CH161 samples for the effects of water softeners. Lastly, the barium which is normally found in neighboring wells at ~0.1ppm is not detected in CH155. Combined with the high sulfate content of the water, this could indicate precipitation of a barite scale (BaSO_4) at the bottom of the well bore, or somewhere in the water lines. Barite is very difficult to remove after it forms. However, it is possible barium does not occur where the Barn's Sink well is completed, or is so minor the barite scale is inconsequential.

Samples CH156 and CH157 are mostly typical of this sample set. They are from very similar sources and the slight differences in their chemistry can provide a sense of the natural error in all analysis. These samples are distinctive for their higher alkalinity, calcium, magnesium, and silicon. These are probably a result of slightly more acidic conditions in the reservoir the well accesses. These acidic conditions can result in greater calcite and dolomite dissolution, and maintain more silica in solution. Due to sample blinding, neither the on-campus student lab, nor CEGR's usual lab was aware of the close relationship between these samples. The near-exact reported concentrations lend high confidence to the analysis of these and all samples in this set. The areas of greatest error appear to be in sulfate, but even in that worst-case are barely more than 2ppm, or ~8% of the measurement.

Sample CH158 was anomalously warm, even after running for a short time to ensure a representative sample. This is most likely due to a mechanical installation, routing through the warm house, or a heated foundation. It is possible the water sources from a small natural geothermal feature, but if so, the salt content of the water is surprisingly low. Water that has been 10degrees Celsius hotter than neighboring waters for a long time would normally dissolve more salts from the reservoir rock. This is because hot water can hold more dissolved salts more than cold water (with a few notable exceptions among the carbonates). Because CH158, like CH153, is otherwise typical of this sample set, it seems likely that the increase in temperature was sudden, anthropogenic, and occurred within a few tens of feet of the faucet, probably isolated from reservoir rock within a plastic pipe, galvanized pipe, or stainless steel pipe.

Samples CH159 and CH161 are samples collected before and after water is run through a water softener. CH159 has the same typical features as CH158 and CH153. When that typical water is run through a water softener a resin populated with sodium ions preferentially pulls calcium, magnesium, and some potassium ions out of solution. Because the water must have a net-zero charge, sodium ions are contributed from the resin back to the water at a roughly 2-to-1 ratio. The combined effect is an exchange of calcium and magnesium ions for sodium ions. During a

recharge cycle the sodium is supplied from a sodium chloride salt, and the captured calcium chloride and magnesium chloride washed off the resin for disposal. The water softener attached to CH161's is working well, probably because it is new and recently loaded with fresh salt, and removes so much calcium and magnesium from the well water that CEGR and the on-campus laboratory machines can no longer detect these ions. The increase in sodium also supports the interpretation that the main difference in these samples is from a water softener. In addition to the aesthetic reasons to exchange calcium and magnesium for sodium, sodium stays in solution better, and is less likely to scale pipes when heated.

CH: Rare Earth Element findings

Samples for Rare Earth Elements from the CH sample set were collected too late in the project to be sent to INL for REE analysis. Because the waters meet domestic drinking water standards and are low salt content, it is unlikely they would have had significant REEs.

CH: Metagenomic findings

Samples for metagenomics at CH are in storage until a later project with suitable funding can make use of them. The samples are stored at -40C to ensure both that the RNA does not deteriorate and that viable cells are unable to continue growth, distorting the sample..

CH: Isotope findings

Samples for isotope analysis at UWyo's SIF were collected but have not been sent to SIF for analysis. Future work may send these samples for analysis.

NF findings at PRB2

Nanofiltration (NF) is a membrane separation technique in which a hydrostatic pressure is applied to pass water through the membrane while other compounds are retained. NF membranes are predominantly made of polymeric thin films with pore size in the range of 2-10 nm. The separation efficiency of NF membranes is determined by the pore size and surface charge of the membrane.⁹ Membrane Pore size affects the sieving separation mechanism which retains compounds bigger than the pore size of membrane. On the other hand, membrane surface charge could be either positive or negative depending on the pH of the feed solution.

Two main factors that describe NF performance are the flux of clean water, permeate flux, and rejection of the solutes. Membrane properties such as pore size, porosity and hydrophilicity determine permeate flux, while pore size and surface charge affect rejection of the contaminants.

⁹ D.L. Oatley-Radcliffe, M. Walters, T.J. Ainscough, P.M. Williams, A.W. Mohammad, N. Hilal, Nanofiltration membranes and processes: A review of research trends over the past decade, J Water Process Eng, 19 (2017) 164-171.

Membrane fouling is the main concern in nanofiltration which results in higher energy demand, increased cleaning and reduced life-time of the membrane.¹⁰ Fouling can occur on the membrane surface as cake layer or inside the pores of the membrane.

NF procedure and instrument settings

A cross-flow nanofiltration system was used to concentrate produced water samples. Figure 19 shows the schematic illustration of the system. Feed solution is pumped to pass over the membrane through the membrane module. The transmembrane pressure was regulated using needle valves before and after the membrane module. The operating pressure was set to be 110 psi. While the feed stream passes over the membrane, water passes through the membrane due to the pressure difference. In the cross-flow operation mode, tangential flow of the membrane creates a shearing effect on the surface of the membrane and helps reduce fouling. An NFG Snyder NF membrane from Snyder Filtration, USA, was used in this study. Figure 19 shows the Zeta potential vs pH of the membrane. The isoelectric pH of the membrane was found to be 4.5, below which the membrane surface has a positive charge. As the REEs have multi-valent positive charge, feed pH was set to be lower than 4.5 to have a positive charge on the membrane surface and thereby retain the REEs. Also, as the lowest tolerable pH for the membrane was 4, feed pH was set to be 4-4.5 using hydrochloric acid (HCl). The active area of the membrane was 42 cm². Permeate flux (LMH, L/m² h) was calculated by measuring the permeate volume during a specific time and was calculated based on the following equation.

$$J = V/A\Delta t$$

where V is permeate volume (L), A is membrane active area (m²) and Δt is time (h). 10 ml of feed and permeate streams were collected every 0.5-1 h to measure REEs concentration and determine their rejection by the membrane using the following equation:

$$Rejection = 1 - C_p/C_f$$

Where C_p and C_f are the concentration in permeate and feed stream, respectively.

¹⁰ N. Hilal, H. Al-Zoubi, N.A. Darwish, A.W. Mohammad, M. Abu Arabi, A comprehensive review of nanofiltration membranes: Treatment, pretreatment, modelling, and atomic force microscopy, *Desalination*, 170 (2004) 281-308.

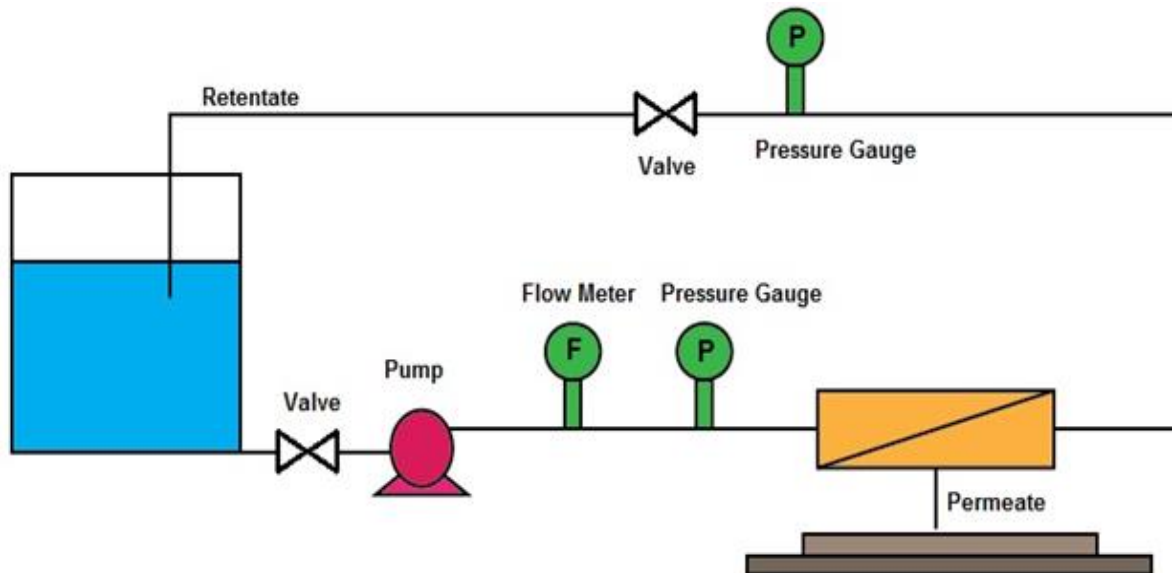


Figure 19: Schematic illustration of cross-flow nanofiltration system.

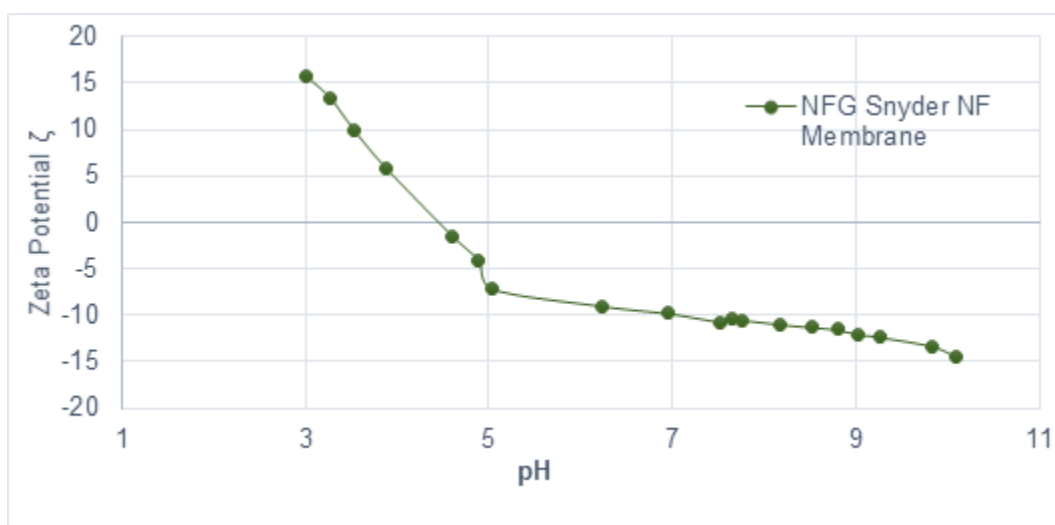


Figure 20: Zeta potential vs pH of NFG Snyder NF membrane.

NF results

The NF procedure described above was used to concentrate REEs in three different PW samples. Two liters of samples were used in all experiments running for around 5 hours. Results are reported as the permeate flux (LMH) vs time, *Figure 20*. The average permeate flux for the hybrid sample, sample 86 and sample 97 was 45.97 ± 1.99 , 37.26 ± 3.28 and 40.85 ± 1.98 LMH, respectively.

The differences in permeate flux could be due to the differences in the composition of feed solutions. The contaminants in the samples results in clogging/fouling and affects the permeate

flux of the membrane. No significant fouling, however, was observed as the permeate flux was stable during the experiment. All tests were conducted under the operating pressure of 110 psi and room temperature.

Figure 22 shows the SEM images of the membrane after the experiments. After hybrid sample treatment, the membrane showed slightly lower fouling than other two experiments with produced waters. In fact, the contaminants in real produced water samples resulted in more fouling and subsequently a lower flux compared to the hybrid sample.

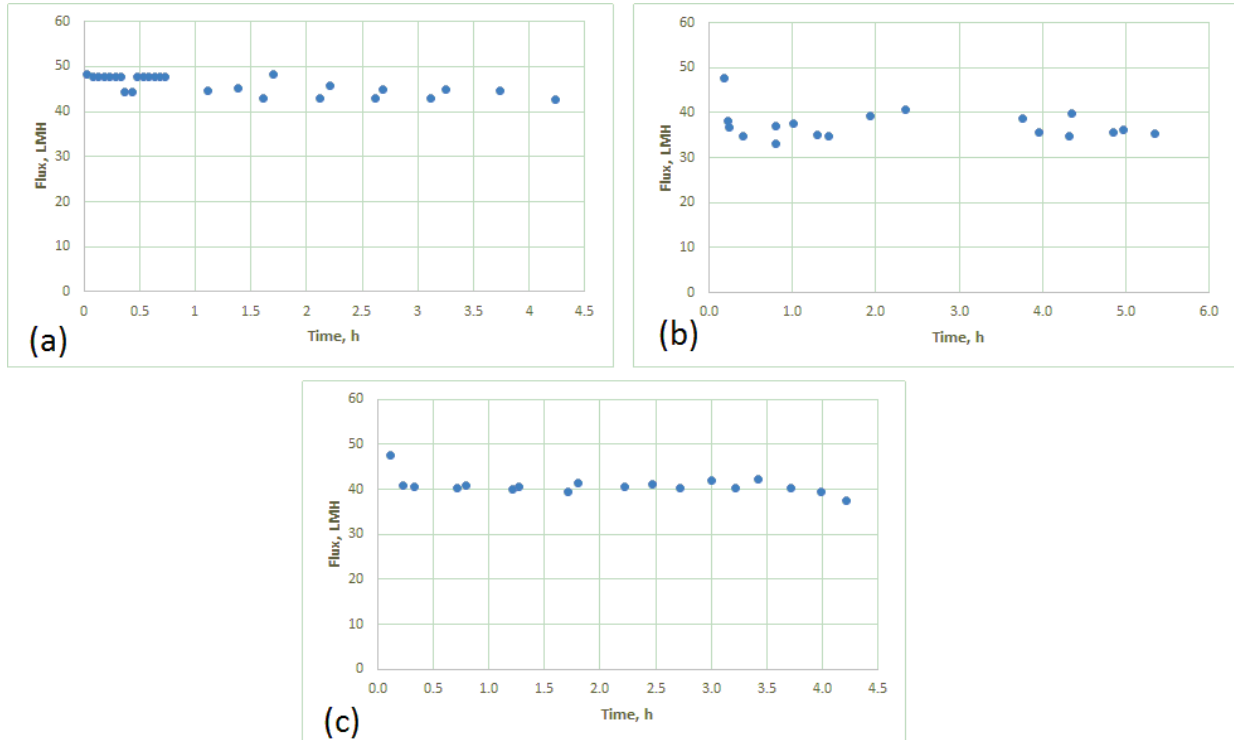


Figure 21: Permeate flux vs running time for (a) hybrid sample, (b) sample 86 and (c) sample 97.

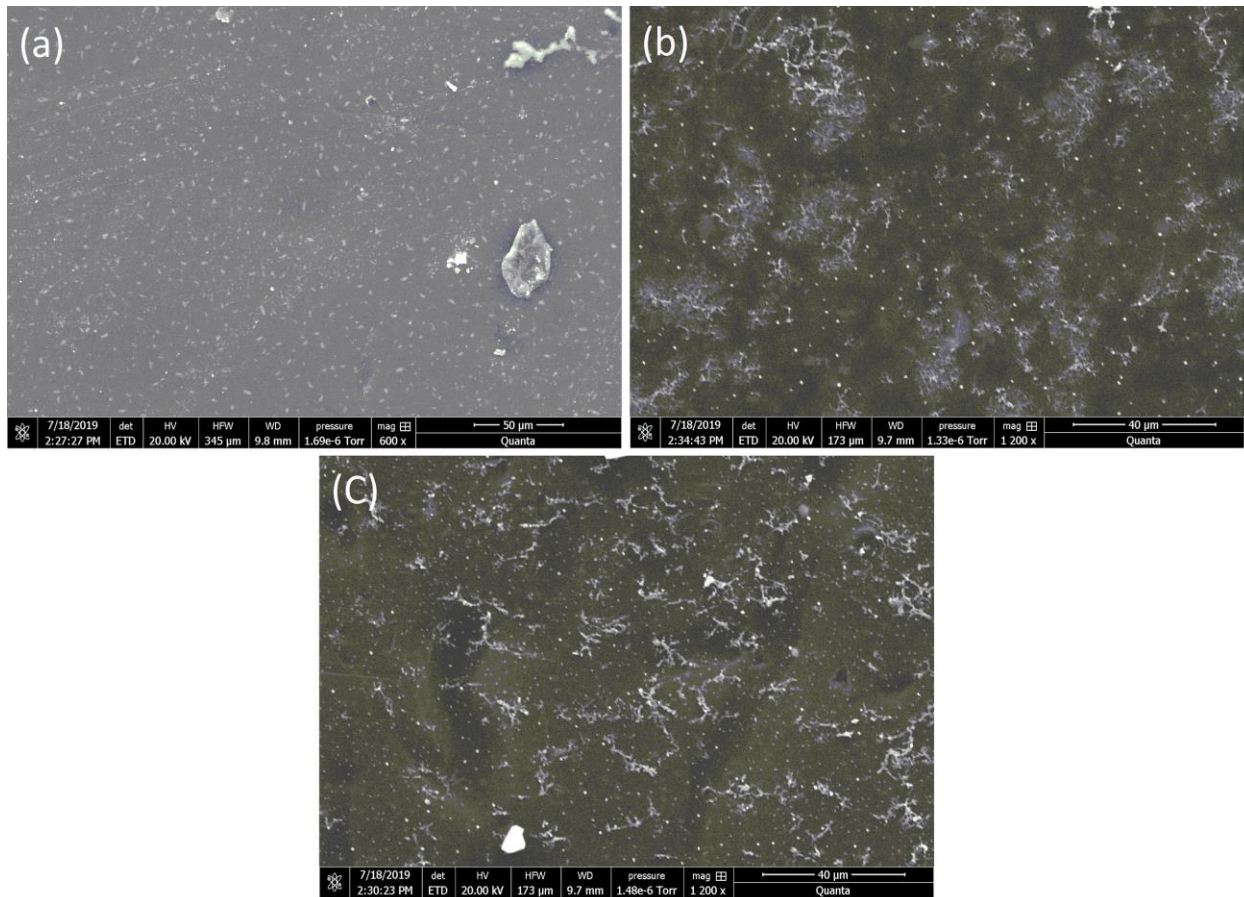


Figure 22: SEM images of the membrane after treating (a) hybrid sample, (b) sample 86 and (c) sample 97. Each shows minor salt accumulation, and samples 86 and 97 show the accumulation of organics.

Samples 97, 86, and H1 (H1 is a blend of produced waters from Wyoming’s Green River Basin) were tested on the NF system and samples of permeate (P in the sample names) and feed solution (F in the sample names) were collected every 30 minutes for four hours. This produced an estimate of their performance lowering the salt content of produced waters. These samples are presented in the appendix with a numeric suffix indicating the time of collection from the start of the test (“0” to the end of the test “8”).

In each of these three tests the result was the same: NF reduced the ionic concentration of all species and could have achieved arbitrarily high performance given adequate pressure and chaining of the cleaned water output as input to the next cycle of NF. The two exceptions to this performance were Iron and Silicon. Silicon content in the feed solution increased continuously, but the permeate was constant. This suggests silicon was blocked by the NF membrane and due to its low concentration increased noticeably in the feed solution over 4 hours. Likewise, more and more iron was found in the feed solution as time passed, but decreased in the permeate solution. This suggests iron was blocked by the NF membrane and that

the pH adjustments to the machine may have dissolved the machine's steel tubing. As both Si and Fe remained at very low concentrations, these two elements are not expected to present a serious obstacle to any NF-treatment technique.

Significance

This work has produced four sample sets all using the same methods and procedures. By sharing these methods and procedures with the "PRB" work which inspired this study, a very large body of data has been produced which can be compared internally. These data produced have already produced presentation and publication opportunities for the students involved. These data are expected to be used by future students to continue the insight they have produced.

The NF experiments have shown that NF membranes in flow-by orientation are resistant to fouling by oil droplets and salts in produced waters. This and the evidenced reduction in salt content suggests that NF could be used in serial configuration to produce a water of arbitrarily high quality, if adequate pressure can be supplied.

The team's past history of working together allowed endurance through the challenges of SARS-CoV-2 and on-time completion of all analyses. This was possible in large part to the familiarity the team members had from past projects together. Future work using this team could continue to benefit from that familiarity.

This work provides many opportunities for future work. The data are suitable for many visualization and statistical testing methods. The data could be resampled in the future to learn which change over time has occurred over the years between the inspirational "PRB" study, this study, and the resampling study. Future partnership with a University of Wyoming expert in extractive chemistry could attempt to electrowin or extract REEs from the NF-concentrate solution.

Acknowledgement and Contributions

This report was edited together from the works of the indicated students and researchers. Some data in the appendixes has appeared in other publications, and are reproduced with permission here. The text for NF was provided by M. Shahabadi. This work would not have been possible without the generous hosting and access provided by Wyoming landowners and industrial partners.

Publications

- Nye, C. “New Data from an Old Well: Changes in the Chemistry of Runoff Geothermal Well Water,” April 2020, World Geothermal Congress 2020. (delayed due to SARS-CoV-2) <https://pangea.stanford.edu/ERE/db/WGC/papers/WGC/2020/14005.pdf>
- Zaixing Huang, M. Fan, D. Bagley, M.A. Urynowicz, Nye, C, et al.. “Anaerobic treatment and energy recovery of produced water from petroleum production using activated sludge from a brewery wastewater treatment facility” (submitted)
- Drogos, D.L., Nye, C., Quillinan, S., Urynowicz, M.A., Wawrousek, K., “Microbial communities in oil and gas produced water from unconventional wells in the Powder River, Wind River, and Green River Basins, Wyoming,” manuscript in preparation.
- Drogos, D.L., Nye, C., Quillinan, S., Urynowicz, M.A., Wawrousek, K., “Differing Microbial Communities from Similar Deep Subsurface Environments in Two Unconventional Oil Wells in the Wyoming Powder River Basin,” manuscript in preparation.
- K. Wawrousek, C. Nye, D. Astling, D. Drogos, S. Quillinan, “Comparative Analysis of Microbial DNA Isolated from Unconventional Wells of the Powder River and Greater Green River Basins.” (submitted)

Presentations

- Mahdi Shahabadi, formerly a PhD candidate in civil & architectural engineering, published and presented a poster at the Wyoming Water Association Annual Meeting and Educational Seminar (October 26, 2018) titled “Nano-Filtration for Treatment of Produced Water and Rare Earth Element Pre-Concentration”. Mahdi Shahabadi was advised by Dr. Jonathan Brant and during the 2018-2019 school year, was funded through this project.
- Nye, Charles and Mahdi Shahabadi (2019) Water Chemistries Associated with Light and Heavy Oils in the Powder River Basin and Laramie Basin, Wyoming. GSA Abstracts with Programs. 51(5). <http://dx.doi.org/10.1130/abs/2019AM-339606>
- Aspen Golding, an undergraduate in chemical engineering, published and presented a poster at University of Wyoming’s Undergraduate Research Day (April 27, 2019) titled “Microbial Communities Composition in Water Samples from a Geothermal Well”. Aspen Golding is advised by Dr. Karen Wawrousek, and co-advised by Charles Nye.
- Nunzio Carducci, an undergraduate in chemical engineering, published and presented a poster at a meeting of the Rocky Mountain Branch of the American Society of Microbiology (May 4, 2019) titled “Microbial Community Composition in Water Samples from a Geothermal Well”. Nunzio Carducci is advised by Dr. Karen Wawrousek, and co-advised by Charles Nye.

Student Support

Student support in this project is described in Figure 1 above, and expanded below in Figure 23.

Student involved	Samples provided	Funding Provided	Publications	Presentations
Shahabadi	PRB2, Hybrid, QD	Fall 2018 - Spring 2019	GSA2019	WWA2018 and GSA2019
Drogos	QD		Yes	Laramie Engineers Club
Golding	DS			Undergraduate Research Day
Carducci	DS			Undergraduate Research Day
Zaixing	Hybrid		Journal of Hazardous Materials	
Phuoc	Hybrid			
Analytical methods class	CH			

Figure 23: Students (some now graduated) who were either funded or supported with samples as part of this work. Work after the end of this study will hopefully include analysis of the data in the appendix as there is much more to be gained from those data. This is expected to allow other students to benefit from the work and to leverage this work to get further funding.

Appendix

All Isotope ratios are in per mil notation. Geochemical concentrations are in mg/kg. Rare Earth Elements are in ng/l. Other units such as pH, ORP, or Temperature are as indicated.

Appendix A: Sample Stable Isotope Ratios

Sample ID	$\delta^{13}\text{C}$	δD	$\delta^{18}\text{O}$	Sample ID	$\delta^{13}\text{C}$	δD	$\delta^{18}\text{O}$
PR2-70		-129.7	-17.49	QD-93	-6.0	-137.6	-19.01
PR2-71	4.0	-51.4	-0.45	QD-94	16.1	-133.8	-17.68
PR2-72	2.1	-61.5	-4.87	QD-95	-14.2	-140.8	-19.08
PR2-73	1.0	-62.1	-5.05	QD-96	-10.8	-141.1	-19.14
PR2-74	-0.6	-62.5	-5.00	QD-97	-13.9	-140.5	-19.01
PR2-75	6.6	-50.2	-0.59	QD-98	-5.7	-140.3	-19.17
PR2-76	-8.3	-55.2	-3.04	QD-99	12.3	-139.4	-18.95
PR2-77	4.1	-53.1	0.02	QD-100	-0.2	-140.2	-18.56
PR2-78	3.7	-59.7	-1.56	QD-101	-15.6	-140.7	-18.87
PR2-79	-5.7	-59.3	-3.74	QD-102	15.1	-141.5	-19.08
PR2-80	-6.4	-55.7	-3.26	QD-103	-16.3	-141.4	-18.84
PR2-81	8.1	-73.6	-4.72	Blank-104	-13.8	-129.9	-17.27
PR2-82	-6.5	-65.8	-4.48				
PR2-83	3.1	-48.3	1.19	Sample ID	$\delta^{13}\text{C}$	δD	$\delta^{18}\text{O}$
PR2-84	-9.8	-65.6	-4.13	DS-62	18.7	-123.5	-16.60
PR2-85	2.5	-47.4	1.47	DS-63	17.6	-73.3	-5.15
PR2-86	20.5	-48.2	1.84	DS-64	18.7	-121.5	-15.92
PR2-87	-7.6	-47.6	0.03	DS-65	18.7	-122.3	-16.30
PR2-88		-49.3	1.85	DS-66	1.8	-131.1	-17.85
PR2-89	5.0	-47.7	1.63				
PR2-90	7.2	-47.5	1.70				
PR2-91		-54.6	0.58				

Appendix B: Sample Geochemistry (mg/L unless otherwise noted)

Sample ID	pH	Cond mS/cm	Temp C	ORP mV	Alkalinity, Total as CaCO3	Bromide	Calcium	Chloride	Fluoride
Blank-70					ND	ND	ND	ND	ND
PR2-71	5.7	55	43.5	46	371	203	613	19400	ND
PR2-72	7.24	36.6	47.3	-34	930	152	73	11400	ND
PR2-73	7.04	36.4	37.6	3	959	152	77	11300	ND
PR2-74	6.76	34.88	41.2	0	850	150	78	11600	ND
PR2-75	6.05	58.6	38.3	9	431	244	673	23100	ND
PR2-76	6.87	34.5	46	12	1080	108	74	10100	ND
PR2-77	5.8	60.9	27.3	103	439	278	896	24600	ND
PR2-78	6.12	55.1	27	57	415	239	684	19600	ND
PR2-79	6.71	30.6	26	-40	1140	91	72	8560	ND
PR2-80	6.42	30.92	20.2	-1	1060	108	82	9690	ND
PR2-81	5.97	43.4	31.7	5	566	123	303	14800	ND
PR2-82	6.84	24.2	44.7	-17	1730	81	41	6650	ND
PR2-83	5.8	79.4	37.1	13	266	315	1260	32200	ND
PR2-84	6.5	29.5	30	-62	1410	88	73	9360	ND
PR2-85	5.59	80.8	44	11	256	343	1200	33200	ND
PR2-86	6.4	59.06	23.5	-101	ND	226	810	24500	ND
PR2-87	6.2	72.16	31.9	-11	454	447	321	25300	ND
PR2-88	5.26	59.7	32.6	16	134	286	771	21600	ND
PR2-89	5.28	74.7	40	56	132	395	1800	29000	ND
PR2-90	6.1	66.9	42.4	-21	198	321	1350	27200	ND
PR2-91	5.1	68.2	30.4	80	98	331	1490	27800	ND
QD-93	5.25	7.947	15.5	-192	426	0.3	2	59	5.4
QD-94	6.43	0.0255	12.5	-80	1580	4.6	17	607	3.1
QD-95	7.63	5.407	11.1	-267	395	0.4	125	606	1.5
QD-96	2.3	8.86	28.3	27	ND	2	394	3770	ND
QD-97	6.28	6.92	29.8	-303	362	0.5	341	656	1.6
QD-98	6.37	2.15	31.5	-300	421	0.4	166	658	1.9
QD-99	5.8	0.82	15.1	-174	501	0.4	5	173	1.7
QD-100	5.24	0.581	11.3	-127	370	0.3	2	100	1.9
QD-101	6.23	0.803	13.4	-240	261	0.6	505	1120	1.3
QD-102	5.42	1.734	11.8	-122	367	0.2	7	43	1.3
QD-103	5.85	3.129	10	-237	420	0.9	404	1130	1.1
Blank-104	6.97	0.04689	8.4	56	ND	ND	2	2	ND
DS-62	7.4	4.698	31.1	-36	2080	1	3	107	3.6
DS-63	8.81	80	17.7	13	4390	32	18	11000	ND
DS-64	8.3	11.3	27.2	22					
DS-65	8.15	4.178	29.4	8	1840	0.9	4	103	3.4
Blank-66									
CH-151	8.04	0.9361	6.5	251	215	ND	81	5	0.3
CH-152	8.04	1.864	8.3	256	166	ND	73	1	0.2
CH-153	8.12	0.4598	8.7	263	176	ND	61	4	0.2
CH-154	8.03	1.811	6.5	120	270	ND	93	5	0.3
CH-155	8.22	0.9289	4.8	40	277	ND	23	6	0.6
CH-156	7.92	0.7419	6.8	198	375	ND	102	3	0.2
CH-157	7.9	0.756	3	210	376	ND	102	3	0.2
CH-158	8.05	1.07	16.2	239	286	ND	86	5	0.2
CH-159	8.02	1.075	7.4	192	222	ND	69	3	0.2
Blank-160									
CH-161	8.1				223	ND	ND	3	0.2

Sample ID	Magnesium	Nitrogen, Ammonia as N	Nitrogen, Nitrate As N	Nitrogen, Nitrite as N	Potassium
Blank-70	ND	ND	ND	ND	ND
PR2-71	42	28	ND	ND	57
PR2-72	16	9.3	ND	ND	30
PR2-73	18	9	ND	ND	39
PR2-74	17	9.5	ND	ND	36
PR2-75	101	42	ND	ND	52
PR2-76	14	8.1	ND	ND	73
PR2-77	85	40	ND	ND	82
PR2-78	62	26	ND	ND	74
PR2-79	12	7.5	ND	ND	40
PR2-80	15	8.1	ND	ND	49
PR2-81	44	82	ND	ND	53
PR2-82	8	77	ND	ND	84
PR2-83	145	47	ND	ND	679
PR2-84	15	7.9	ND	ND	88
PR2-85	138	46	ND	ND	335
PR2-86	80	32	1730	ND	170
PR2-87	45	27	6	ND	78
PR2-88	58	50	ND	ND	49
PR2-89	131	44	ND	ND	193
PR2-90	96	46	ND	ND	277
PR2-91	109	42	ND	ND	204
QD-93	ND	0.22	0.1	ND	ND
QD-94	3	ND	ND	ND	7
QD-95	34	0.26	ND	ND	20
QD-96	62	28	ND	ND	42
QD-97	40	0.33	ND	ND	19
QD-98	25	0.59	ND	ND	13
QD-99	ND	0.14	ND	ND	1
QD-100	ND	0.2	ND	ND	ND
QD-101	66	0.54	ND	ND	25
QD-102	ND	ND	ND	ND	ND
QD-103	37	0.55	ND	ND	54
Blank-104	ND	ND	ND	ND	ND
DS-62	ND	0.78	ND	ND	3
DS-63	1000	0.09	ND	ND	247
DS-64					
DS-65	ND	0.71	ND	ND	4
Blank-66					
CH-151	21	ND	0.3	ND	3
CH-152	24	ND	ND	ND	3
CH-153	15	ND	0.1	ND	3
CH-154	22	ND	ND	ND	4
CH-155	7	0.15	ND	ND	2
CH-156	28	ND	ND	ND	4
CH-157	29	ND	ND	ND	4
CH-158	19	ND	ND	ND	4
CH-159	13	ND	0.1	ND	3
Blank-160					
CH-161	ND	ND	0.1	ND	ND

Sample ID	Sodium	Sulfate	Aluminum	Arsenic	Barium	Boron	Iron	Manganese	Molybdenum	Silicon	Strontium
Blank-70	1	ND	ND	ND	ND	ND	ND	ND	ND	ND	ND
PR2-71	11700	ND	ND	0.003	41.9	24	0.52	0.79	0.018	33	60.6
PR2-72	7200	ND	0.07	ND	20.7	14.1	ND	0.048	0.001	21	17.5
PR2-73	8240	ND	ND	ND	18.7	14.9	ND	0.073	ND	22	18.1
PR2-74	7920	ND	ND	ND	20.3	15	ND	0.075	ND	19	17.2
PR2-75	12800	50	ND	0.002	98.8	21	0.21	0.54	0.01	28	93.2
PR2-76	6820	ND	ND	ND	18.7	13	ND	0.044	ND	23	16.3
PR2-77	13800	ND	0.04	0.002	97	30	0.36	15.2	0.023	32	118
PR2-78	12200	ND	0.03	0.002	72.3	31	0.11	9.51	0.019	53	86.3
PR2-79	6100	ND	ND	ND	13.7	13.4	ND	0.164	0.002	21	14.6
PR2-80	6710	ND	ND	ND	16.7	12.8	ND	0.095	ND	23	16.8
PR2-81	9330	ND	ND	ND	58.5	17.3	12.7	2.27	0.006	10	46.8
PR2-82	5420	9	0.05	ND	10.9	14	6.8	0.148	ND	21	8.52
PR2-83	18300	ND	ND	ND	212	24	4.7	0.931	ND	31	188
PR2-84	6650	ND	ND	ND	20.6	14	2.01	0.084	0.002	23	16.6
PR2-85	18800	ND	0.08	0.013	242	20	21.2	1.27	0.002	40	165
PR2-86	13200	ND	ND	ND	48	31.2	79	2.67	ND	19	104
PR2-87	15000	ND	ND	ND	151	20.4	0.19	0.29	0.005	27	82.7
PR2-88	13200	79	0.8	0.009	3.3	30	110	1.42	0.011	54	83
PR2-89	16600	ND	ND	ND	190	17	3.14	1.25	0.006	41	262
PR2-90	14200	ND	ND	0.001	143	17	0.31	1.37	0.018	38	209
PR2-91	15700	ND	0.04	ND	139	15	29.4	1.58	ND	33	227
QD-93	268	16	0.03	0.003	1.36	1.06	0.24	0.02	ND	11.5	0.13
QD-94	1170	ND	ND	ND	1.16	2.5	0.03	0.112	0.003	11.8	0.66
QD-95	690	326	ND	ND	0.28	0.97	0.09	0.018	ND	13.4	5.76
QD-96	1640	1370	0.1	ND	0.15	1.4	59.1	0.362	0.005	13.3	12.6
QD-97	715	801	ND	ND	0.11	1	0.18	0.009	ND	13.8	9.39
QD-98	725	478	0.08	ND	0.54	1	0.11	0.084	ND	13.2	5.37
QD-99	366	3	ND	0.001	0.38	0.75	0.05	0.119	ND	11.5	0.1
QD-100	269	18	0.03	ND	0.59	0.69	0.04	0.012	ND	11.6	0.09
QD-101	1090	1370	ND	ND	ND	1.3	0.05	0.02	ND	14.9	14.4
QD-102	210	7	0.03	ND	1.61	0.46	ND	0.382	ND	12.5	0.14
QD-103	1520	1880	ND	ND	0.06	1.9	ND	0.074	ND	17	10.3
Blank-104	3	3	ND	ND	ND	ND	0.03	ND	ND	0.1	0.02
DS-62	887	2	ND	ND	1.53	ND	ND	0.003	0.001	9	0.52
DS-63	27900	38000	ND	0.036	0.09	9.8	0.1	0.005	0.028	2	5.44
DS-64											
DS-65	1020	ND	ND	ND	1.85	ND	ND	0.003	ND	10	0.6
Blank-66											
CH-151	13	84	ND	ND	0.05	ND	ND	0.002	0.002	11.9	0.49
CH-152	12	127	ND	ND	0.05	ND	ND	0.002	0.002	8.2	0.5
CH-153	14	50	ND	0.001	0.06	ND	ND	0.002	0.001	10.9	0.24
CH-154	49	128	ND	ND	0.09	ND	0.04	0.073	0.001	11.9	0.34
CH-155	206	195	ND	ND	ND	0.25	ND	0.072	0.001	4.5	0.29
CH-156	26	31	ND	ND	0.15	0.07	ND	ND	ND	13.6	0.45
CH-157	25	31	ND	ND	0.15	0.06	ND	0.001	ND	13.7	0.45
CH-158	26	36	ND	ND	0.15	ND	ND	ND	ND	12.5	0.52
CH-159	15	25	ND	ND	0.1	ND	ND	ND	0.001	12.2	0.4
Blank-160											
CH-161	122	25	ND	ND	ND	ND	ND	ND	0.001	12	ND

Appendix C: Sample REE concentrations (ng/L)

Samples	Sc	Y	La	Ce	Pr	Nd	Sm	Eu	Gd	Tb	Dy	Ho	Er	Tm	Yb	Lu
DS-62	1.95	11.11	2.02	2.92	0.27	0.96	0.17	7.23	0.30	0.10	0.84	0.25	0.93	0.16	1.06	0.17
DS-63	21.75	50.48	17.80	57.21	4.04	19.57	3.84	1.69	3.74	0.70	5.39	1.48	5.95	1.13	9.37	1.71
DS-64	3.87	15.71	4.52	5.33	0.32	1.39	0.26	14.69	0.44	0.12	1.08	0.33	1.33	0.23	1.70	0.26
DS-65	0.59	2.38	0.66	1.12	0.09	0.45	0.02	0.93	0.05		0.10	0.03	0.15	0.02	0.18	
PRB2-70		0.09	2.59	0.26		0.07	0.73	0.06								
PRB2-71	45.21	2.71	48.67	42.67	0.46	2.74	0.32	246.96	0.40	0.04	0.23	0.04	0.18		0.27	0.02
PRB2-72	17.02	26.18	5.93	6.12	0.32	1.71	0.66	13.70	1.50	0.46	4.58	1.10	3.51	0.47	2.97	0.38
PRB2-73	14.61	30.17	15.87	15.66	0.34	1.64	0.61	8.67	1.39	0.42	4.65	1.19	3.96	0.53	3.28	0.43
PRB2-74	12.86	27.47	8.54	10.89	0.25	1.55	0.80	9.42	1.88	0.48	4.63	1.16	3.76	0.49	3.12	0.40
PRB2-75	33.49	1.73	13.36	7.58	0.14	1.58	0.11	58.48	0.11	0.02	0.09		0.07		0.07	
PRB2-76	21.61	10.24	10.09	12.58	0.43	2.04	0.40	48.51	0.53	0.10	0.88	0.21	0.75	0.10	0.76	0.10
PRB2-77	77.39	25.61	16.59	147.23	1.93	11.01	4.53	106.90	6.62	1.22	8.35	1.72	5.03	0.68	4.48	0.62
PRB2-78	67.68	39.85	6.52	8.33	1.88	16.62	10.71	44.54	15.77	2.80	18.13	3.56	9.62	1.17	6.91	0.90
PRB2-79	17.88	4.66	6.01	141.66	0.34	1.45	0.25	31.96	0.38	0.04	0.27	0.05	0.23	0.03	0.24	0.03
PRB2-80	25.49	12.43	6.53	3.73	0.29	1.54	0.41	48.53	0.70	0.12	0.92	0.23	0.84	0.12	0.87	0.13
PRB2-81	63.97	10.90	17.63	8.82	0.16	1.31	0.12	205.01	0.15	0.02	0.15	0.09	0.16	0.03	0.27	0.04
PRB2-82	22.23	13.20	5.61	5.66	0.55	2.69	0.85	37.32	1.56	0.35	2.75	0.59	1.88	0.26	1.76	0.25
QD-93	1.15	4.60	2.79	3.43	0.40	1.54	0.30	6.70	0.45	0.08	0.55	0.12	0.35	0.04	0.25	0.03
QD-94	13.16	29.69	19.63	23.48	3.90	13.61	1.95	6.85	2.31	0.41	2.89	0.68	2.56	0.50	4.76	1.02
QD-95	7.43	10.24	0.19	0.04				2.28							0.08	
QD-96	2.95	138.89	268.25	1285.35	23.70	89.29	13.53	2.71	17.31	2.68	19.12	4.60	16.01	2.47	18.28	3.12
QD-97	11.54	5.99	0.10	0.24				0.50							0.02	
QD-98	9.43	5.08	0.82	0.22		0.07		4.91								
QD-99	1.39	0.61	0.51	0.14	0.02	0.06	0.02	5.51	0.03		0.03	0.02	0.03	0.02	0.04	0.02
QD-100	8.85	3.92	0.06	0.10		0.05	0.03	0.06	0.07		0.06		0.02		0.09	0.06
QD-101	2.89	1.07	2.27	0.30	0.02	0.19		26.60	0.02		0.04		0.05		0.07	
QD-102	0.58	0.60	1.00	0.20		0.09		8.65			0.01		0.02		0.04	
QD-103	10.47	9.01	0.37	0.46	0.04	0.17	0.05	0.12	0.15	0.04	0.50	0.18	0.86	0.15	1.09	0.19

Appendix D: Concentrations of NF samples.

Highlighting indicates analyses outside the instrument's calibration range.

Sample Id	K	Si	B	Na	Ca	Ba	Fe	Mg
97Raw	38.183	9.574	1.812	533.496	258.109		1.579	36.585
97P8	29.069	9.464	1.315	422.836	147.758		1.060	19.970
97P7	28.569	9.529	1.134	425.778	145.267		0.955	20.074
97P6	28.408	9.557	1.027	423.271	146.114		1.166	20.317
97P5	27.822	9.455	0.936	416.214	143.479		1.243	19.970
97P4	28.001	9.591	0.950	427.378	145.254		1.365	20.483
97P3	28.212	9.429	0.905	421.985	144.839		1.578	20.113
97P2	28.101	9.548	0.866	423.114	145.330		1.882	20.580
97P1	27.369	9.454	0.834	416.664	143.074		2.585	20.391
97P0	27.766	8.736	0.738	412.140	151.114			21.219
97F8	39.155	10.183	0.817	568.351	270.640		1.598	38.650
97F7	38.356	10.079	0.769	552.466	266.466		1.556	37.879
97F6	38.167	10.029	0.763	549.070	262.797		1.483	37.131
97F5	38.183	9.910	0.724	529.560	256.912		1.416	36.035
97F4	37.632	9.962	0.731	535.357	254.967		1.358	35.751
97F3	37.103	9.828	0.712	523.877	247.268		1.289	34.827
97F2	36.663	9.716	0.679	512.486	242.742		1.224	34.048
97F1	36.904	9.866	0.688	515.984	240.435		1.154	34.078
97F0	36.673	9.871	0.679	508.536	236.201		1.090	33.570

Sample Id	K	Si	B	Na	Ca	Ba	Fe	Mg
H1Raw	72.479	21.681	11.992	3184.859	68.450			7.723
H1P8	82.813	22.692	10.235	2122.422	42.929	0.142		6.793
H1P7	81.730	22.688	9.936	2096.781	43.033	0.143		6.783
H1P6	82.394	22.883	9.941	2106.946	43.158	0.141		6.865
H1P5	81.338	22.594	9.706	2052.370	42.654	0.140		6.728
H1P4	83.013	22.674	9.693	2040.548	42.794	0.143		6.748
H1P3	81.816	22.448	9.608	2040.395	42.240	0.134		6.680
H1P2	79.494	22.451	9.594	2044.001	42.504	0.134		6.699
H1P1	80.628	22.845	9.734	2057.443	43.216	0.127		6.930
H1F8	70.923	24.277	20.277	3588.062	73.528			8.604
H1F7	67.563	22.908	15.595	3363.941	70.953			8.185
H1F6	65.558	23.563	12.504	3314.109	68.248			7.821
H1F5	64.722	22.226	10.636	3276.154	67.722			7.908
H1F4	63.619	21.912	9.060	3240.993	66.328			7.583
H1F3	62.510	21.801	8.030	3223.577	64.937			7.609
H1F2	63.375	21.970	7.084	3218.797	64.906			7.419
H1F1	62.007	21.973	6.551	3213.580	64.282			9.008
H1F0	61.905	22.516	4.904	3181.359	61.483			6.960

Sample Id	K	Si	B	Na	Ca	Ba	Fe	Mg
86RAW	43.285	10.622	4.780	690.346	159.508			21.156
86P8	21.111	10.754	0.747	506.982	91.388	0.130	0.855	15.472
86P7	20.962	10.610	0.743	505.648	90.836	0.132	0.194	15.216
86P6	21.371	10.580	1.711	505.650	91.026	0.139	0.290	15.406
86P5	20.514	10.542	1.309	496.578	90.394	0.140	0.445	15.734
86P4	20.438	10.608	1.152	491.996	90.022	0.143	0.714	15.712
86P3	20.091	10.525	1.039	484.482	89.138	0.135	1.296	15.546
86P2	20.104	10.548	0.969	483.909	88.927	0.137	1.332	15.535
86P1	20.002	10.533	0.921	469.544	88.763	0.141	0.589	15.434
86P0	21.065	10.174	0.873	514.262	103.276	0.067		17.862
86F8	37.035	9.661		759.552	166.800			22.354
86F7	36.335	9.875		722.491	165.859			22.242
86F6	32.874	9.571		690.601	166.284			22.388
86F5	38.178	9.409		681.466	157.577			21.198
86F4	37.417	9.064		654.218	155.360			20.764
86F3	33.663	8.947		657.751	159.100			21.526
86F2	36.989	8.148		644.571	144.203			18.870
86F1	36.094	8.250		623.494	146.850			19.491
86F0	34.026	8.364		624.439	147.413			19.579